

UNCLASSIFIED

AD 428242

DEFENSE DOCUMENTATION CENTER

FOR

SCIENTIFIC AND TECHNICAL INFORMATION

CAMERON STATION, ALEXANDRIA, VIRGINIA



UNCLASSIFIED

NOTICE: When government or other drawings, specifications or other data are used for any purpose other than in connection with a definitely related government procurement operation, the U. S. Government thereby incurs no responsibility, nor any obligation whatsoever; and the fact that the Government may have formulated, furnished, or in any way supplied the said drawings, specifications, or other data is not to be regarded by implication or otherwise as in any manner licensing the holder or any other person or corporation, or conveying any rights or permission to manufacture, use or sell any patented invention that may in any way be related thereto.

**Best  
Available  
Copy**

428242

CATALOGED BY DDC

AS AD NO. \_\_\_\_\_

428242

# JANAI R

JOINT ARMY-NAVY AIRCRAFT INSTRUMENTATION RESEARCH

## ROTOR BLADE RADAR ANTENNA

PHASE I

REPORT NO. 299-099-251



BELL HELICOPTER COMPANY

FORT WORTH, TEXAS

DIVISION OF BELL AEROSPACE CORPORATION • A **Textron** COMPANY

DDC  
FEB 3 1984  
TISIA A

JANAIR

JOINT ARMY-NAVY AIRCRAFT INSTRUMENTATION RESEARCH

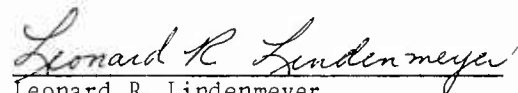
ROTOR BLADE RADAR ANTENNA REPORT  
PHASE I

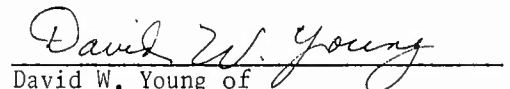
Technical Report

299-099-251

January 13, 1964

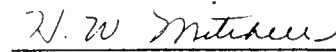
By

  
Leonard R. Lindenmeyer  
Project Engineer

  
David W. Young of  
David W. Young and Associates, Inc.

APPROVED:

  
H. W. Upton  
Chief Electronics Research Engineer

  
H. W. Mitchell  
Chief Electronics Engineer

OFFICE OF NAVAL RESEARCH  
Contract Nonr 4148(00)

This report presents work which was performed under the Joint Army-Navy Aircraft Instrumentation Research (JANAIR) Program, a research and development program directed by the United States Navy, Office of Naval Research. Special guidance is provided to the program from the Army Material Command, the Office of Naval Research and the Bureau of Naval Weapons through an organization known as the JANAIR Committee. The group is currently composed of the following representatives:

U. S. Navy, Office of Naval Research, Committee Chairman

- Lcdr. D. E. Rosenquist

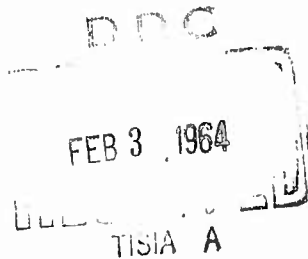
U. S. Navy, Bureau of Naval Weapons

- Cdr. J. E. Perry

U. S. Army, Office of the Chief Signal Office

- Mr. W. C. Robinson

An objective of JANAIR is to improve sensor devices for use in the man-machine complex with all-visibility operating capabilities.



## PREFACE

There are many helicopter missions in which high resolution search and mapping radars are required. There are two desirable features of these radars which are normally incompatible with the limited space, electrical power, and lifting and speed capability of helicopters. The requirements are that the radar have a narrow beamwidth (requiring a long antenna), and a scanning rate of several cycles per second with 20 to 30 cps desirable. These conditions are difficult to obtain because there is no space available for a long antenna; but even if space were available, the power and weight required to spin the antenna would be prohibitive.

One of the most important applications of a rotor blade antenna is in the general field of real time data processing. This is defined as data which is obtained at such a rate and displayed in such a manner, that the data and display will track any maneuver of the helicopter without smearing, jumping, or flickering. With real time data normal visual cues can be maintained.

The above facts led to consideration of the main rotor blade as the antenna. The principle involved the placement of a slotted array antenna in the rotor blade, using the existing rotation of the blade for scanning. A company-funded project was initiated in early 1963 to investigate the problem. The results indicated that the concept of using the main rotor blade of a UH-1B helicopter was feasible. An unsolicited proposal was then submitted to the Office of Naval Research by Bell Helicopter Company with David W. Young and Associated, Incorporated, as a subcontractor. A six-month study contract, Nonr 4148(00), was awarded to Bell.

#### ABSTRACT

A research program, administered by the Office of Naval Research, to investigate the feasibility of using the main rotor blade of a helicopter as a radar antenna was conducted by Bell Helicopter Company with David W. Young and Associates, Incorporated, as a major subcontractor. Special blade sections were built and tested to study various design ideas. Digital computer studies of slotted arrays were programmed on an IBM 7070 computer at Bell. Both a 43-inch section and a 173-inch section of UH-1B rotor blade were built with a slotted array placed near the trailing edge. These blade antennas were statically tested. Radiation pattern measurements were made of beamwidths, sidelobe levels, and front-to-back ratios. The problem of transmitting energy to a spinning rotor blade was examined and preliminary sketches of the hub layout were made. A 0.28 degree beamwidth was obtained at the Rayleigh Range for the 173-inch blade with the antenna focused at infinity. Sidelobe levels and front-to-back ratio were 20 db.



## TABLE OF CONTENTS

	<u>Page</u>
I. INTRODUCTION . . . . .	1
II. ROTOR BLADE ANTENNA DESIGN . . . . .	3
A. Special Blade Sections . . . . .	3
1. Configurations	
2. Test Results	
B. Single and Dual Slot Blade Sections . . . . .	13
1. Configurations	
2. Test Results	
III. THE TRAILING EDGE BLADE ANTENNA . . . . .	22
A. The 43-inch 60-slot Blade Antenna . . . . .	22
1. Configuration	
2. Test Results	
B. The 240-slot Array . . . . .	28
1. Configuration	
2. Test Results	
C. The 173-inch 240-slot Blade Antenna . . . . .	36
1. Configuration	
2. Test Results	
IV. THE BLADE-HUB ASSEMBLY . . . . .	44
V. THE LEADING EDGE BLADE ANTENNA . . . . .	46
VI. CONCLUSIONS . . . . .	48
VII. APPENDICES . . . . .	50
VIII. REFERENCES . . . . .	73
IX. DISTRIBUTION LIST . . . . .	74

# LIST OF ILLUSTRATIONS

<u>Figure</u>		<u>Page</u>
1.	Antenna Pattern for Single Slot, Perpendicular Polarization . . . . .	4
2.	Antenna Pattern for Single Slot, Horizontal Polarization . . . . .	5
3.	Antenna Pattern for Unmounted Multiple Slot Linear Array . . . . .	7
4.	Antenna Pattern for Mounted Multiple Slot Linear Array . . . . .	8
5.	Surface Wave on Long Smooth Surface, Trailing Edge . . .	10
6.	Surface Wave on Long Rough Surface, Trailing Edge . . .	11
7.	Surface Wave on Short Smooth Surface, Trailing Edge . . .	12
8.	Sketch of Trailing Edge Spar for a UH-1B Rotor Blade . .	14
9.	Phased Dual Slot Antenna . . . . .	15
10.	Single Slot Antenna with Maximum Width Trailing Edge . .	17
11.	Single Slot Antenna with Minimum Width Trailing Edge . .	18
12.	Section A, Elevation Radiation Pattern . . . . .	20
13.	Section B, Elevation Radiation Pattern . . . . .	21
14.	Section C, Elevation Radiation Pattern . . . . .	21
15.	43-inch Rotor Blade Section Containing a 60-slot Linear Array . . . . .	23
16.	Drawing of 43-inch 60-slot Trailing Edge Blade Antenna . . . . .	24
17.	Azimuth Pattern for 43-inch 60-slot Trailing Edge Blade Antenna . . . . .	26
18.	Vertical Pattern for 43-inch 60-slot Trailing Edge Blade Antenna . . . . .	26
19.	The Slotted Array . . . . .	29
20.	Slot Offset Distances at 16.15 KMC for 30 db Sidelobes and 5 Per cent Power to the Load . . . . .	33

# LIST OF ILLUSTRATIONS (Continued)

<u>Figure</u>		<u>Page</u>
21.	Azimuth Pattern for the 240-slot Array . . . . .	35
22.	Drawing of 173-inch 240-slot Blade Antenna . . . . .	37
23.	Pieces of 173-inch Blade Antenna Ready for Assembly. . .	39
24.	173-inch Blade Section with One-third of the Slotted Array in the Groove . . . . .	40
25.	173-inch 240-slot Blade Antenna Without Cellfoam . . . .	41
26.	Azimuth Pattern for 173-inch 240-slot Blade Antenna. . .	43
27.	The Blade-Hub Assembly . . . . .	45
28.	Drawing of the Leading Edge Blade Antenna . . . . .	47
29.	In-Plane Blade Deflection Curves at Various Azimuth Positions . . . . .	52
30.	Sketch Showing Variables and Layout for Computer Programs Radar 1 and Radar 2 . . . . .	58
31.	Plot of Antenna Phase Pattern at 4x Rayleigh Range for $N = 50$ . . . . .	61
32.	Plot of Antenna Phase Pattern at the Rayleigh Range for $N = 50$ . . . . .	62
33.	Plot of Antenna Phase Pattern at One-fourth the Rayleigh Range for $N = 50$ . . . . .	63
34.	Plot of Antenna Phase Pattern at One-sixteenth the Rayleigh Range for $N = 50$ . . . . .	64
35.	Plot of Antenna Phase Pattern at 4x Rayleigh Range for $N = 368$ . . . . .	65
36.	Plot of Antenna Phase Pattern at the Rayleigh Range for $N = 368$ . . . . .	66
37.	Plot of Antenna Phase Pattern at One-fourth the Rayleigh Range for $N = 368$ . . . . .	67
38.	Plot of Antenna Phase Pattern at One-sixteenth the Rayleigh Range for $N = 368$ . . . . .	68

LIST OF ILLUSTRATIONS (Continued)

<u>Figure</u>		<u>Page</u>
39.	Plot of Normalized Slot Conductance for a 241-slot Array Having 30 db Sidelobes and 5 Per cent Power to the Load. . . . .	70
40.	Plot of Amplitude Distribution of a 241-slot Array Having 30 db Sidelobes . . . . .	71

## I. INTRODUCTION

This research, conducted jointly by Bell Helicopter Company and David W. Young and Associates, Inc., was undertaken to prove the feasibility of using the helicopter main rotor blade as a radar antenna. Several questions arise in examining the concept: (1) Can a suitable pattern be obtained? (2) What are the effects of blade flapping, bending, coning, etc? (3) What are the aerodynamic, material, stress, reliability, and cost problems of constructing such an antenna? (4) How will the energy be transmitted to the spinning rotor blade?

Several special blade sections were built in which a single slot of an antenna was simulated. The results of tests on these sections were combined with data from the company-funded study to establish a design for a 43-inch 60-slot blade antenna. After testing the 43-inch section, a 173-inch 240-slot blade antenna was built and tested. This report details the results obtained for both a 43-inch and a 173-inch section of UH-1B rotor blade containing a slotted array antenna in its trailing edge.

A study of the motions of the helicopter blade-hub assembly was made. Consideration was given to both blade motion and stabilizer bar motion. A sketch of the hub layout is included to illustrate a method for transmitting energy from the helicopter cabin area to the main rotor blade.

During the period of the above program, a separate research effort at Bell investigated the leading edge erosion problem. The purpose of the program was to find materials which could better withstand the dust and rain erosion that occurs at the leading edge of a rotor blade. The promising results of this materials research made a leading edge antenna feasible. Consequently, a leading edge blade antenna was built late in the

program and is presently undergoing tests. Results will be submitted as an addendum to this report.

## II. ROTOR BLADE ANTENNA DESIGN

The design of the slotted array rotor blade antenna configuration was accomplished by combining the theory of slotted arrays with some experimental test data. The experimental tests were designed to examine the effect of the rotor blade geometry on the antenna characteristics. After studying these data, a design criteria for the array was established, together with the blade antenna configuration.

### A. Special Blade Sections\*

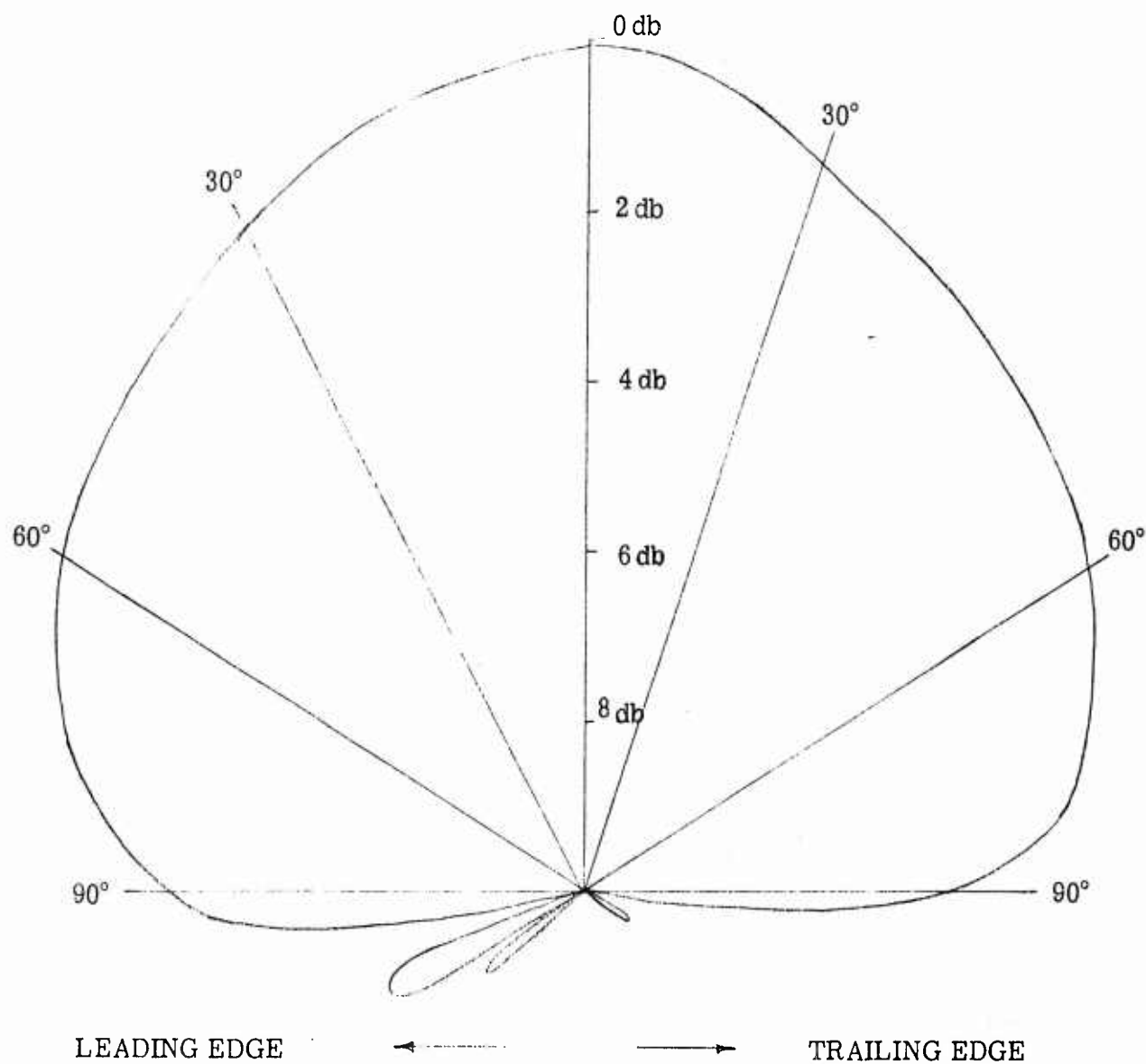
#### 1. Configurations

There are various ways to approach the problem of providing a useful elevation pattern for the rotor blade antenna. To test the severity of the problem, several tests were set up using special blade sections. Actual radiation patterns were measured using a UH-1B rotor blade section. These measurements were made to test the effects of diffraction due to polarization (orientation of the waveguide or slot on the rotor blade), diffraction due to the leading edge of the blade, and diffraction due to the trailing edge of the blade.

Two sections of blade were used to examine the effects of parallel and perpendicular polarization. Single slots were used for convenience only; a slotted array could have also been used. Figures 1 and 2 show the results as well as an illustration of the orientation of the slot in the blade.

A 44-inch 60-slot array was then tested unmounted and mounted on the blade. Perpendicular polarization was used with RG-121U waveguide. The frequency, polarization, and orientation of the array are illustrated in Figures 3 and 4 together with the results.

\*This work was accomplished before receiving the contract from the Office of Naval Research. It is reported here for continuity purposes.



NOTES:

1. Frequency 16.2 KMC
2. E Plane 360° Pattern
3. Perpendicular Polarization
4. Wave Guide RG 91/U

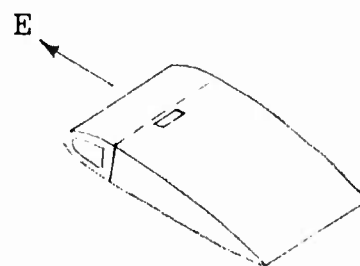
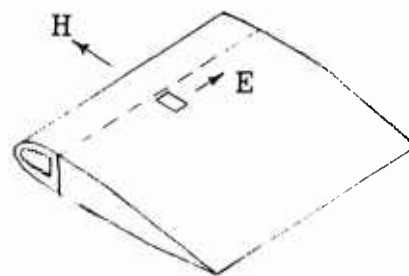
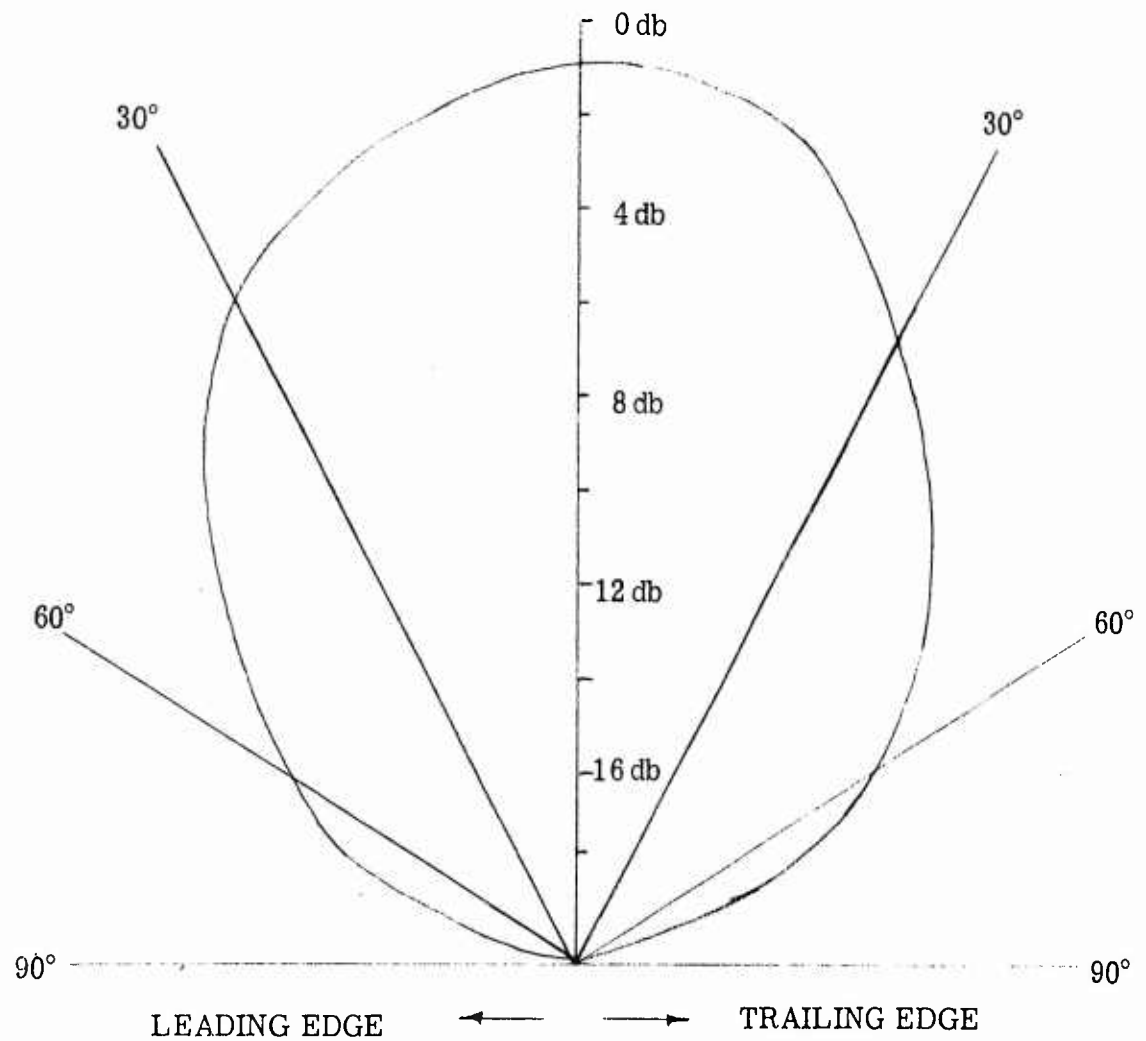


Figure 1. Antenna Pattern for Single Slot, Perpendicular Polarization





NOTES:

1. Frequency 16.2 KMC
2. H Plane 360° Pattern
3. Parallel Polarization
4. Wave Guide RG 91/U

Figure 2. Antenna Pattern for Single Slot, Horizontal Polarization

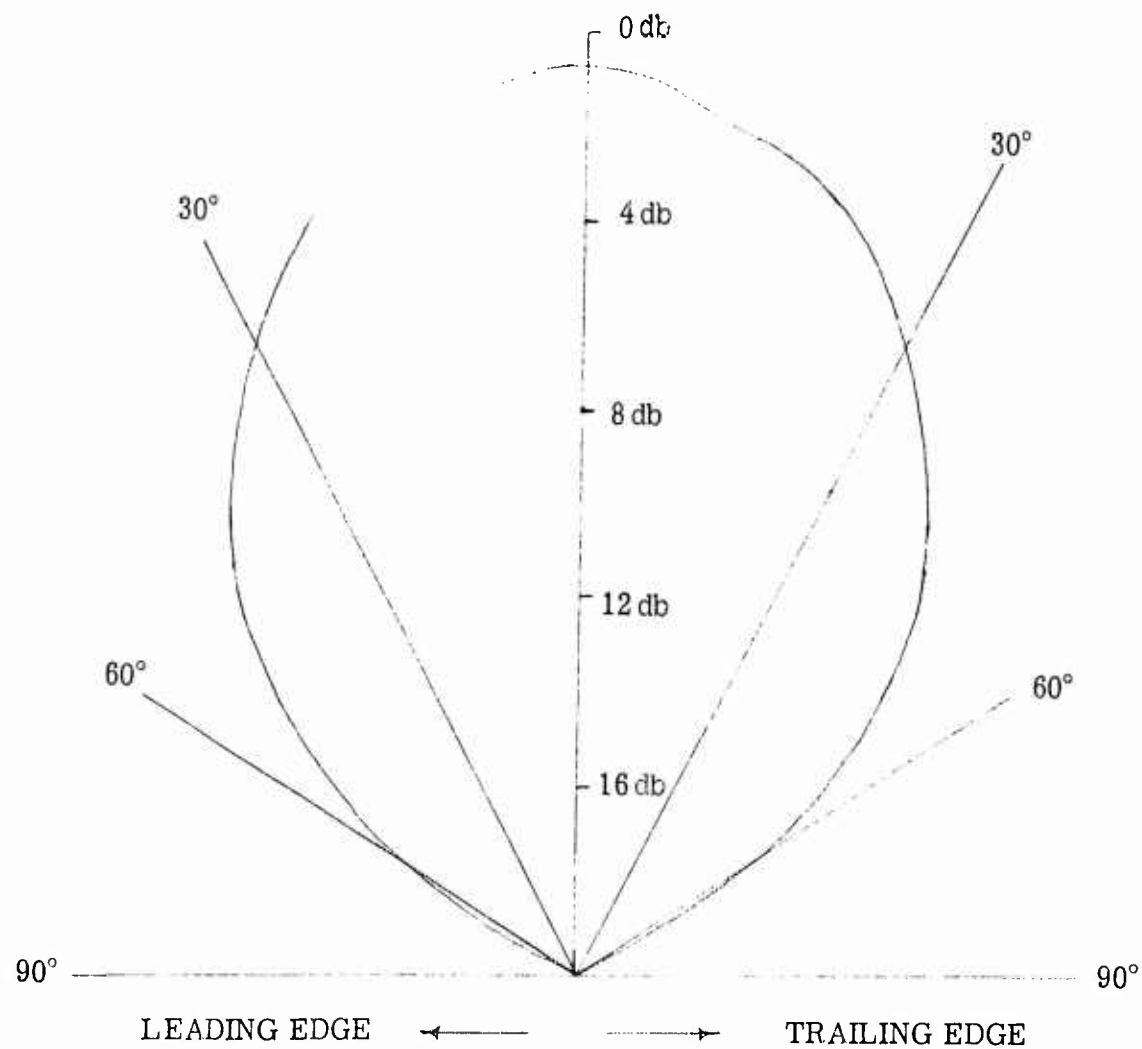
Finally, several sections of blade were modified to examine antenna patterns obtained with a single slot whose aperture opened on to the trailing edge. A single slot antenna was used at a frequency of 16.2 KMC with perpendicular polarization. The sections are illustrated in Figures 5, 6, and 7. Figures 5 and 6 give results with the honeycomb covered and exposed, respectively. The waveguide is mounted close to the box beam. In Figure 7 results are shown for the aperture positioned close to the trailing edge spar.

## 2. Test Results

Vertical polarization, rather than horizontal, gives better diffraction and thus gives a better vertical pattern. The rounded leading edge might give better beam bending characteristics than the sharp trailing edge, but launching a surface wave on the leading edge may be more difficult. The leading edge has not been fully explored (see Section V).

The relative signal strength at one edge of the blade as compared to the other is an important factor, and the front-to-back ratio should be high. Vertical polarization as shown in Figure 1 gives greater radiation coverage and has greater capability for providing radiation around the edges of the blade, but backlobes are present even well around on the back side of the blade. Horizontal radiation as shown in Figure 2 has an excellent front-to-back ratio, but this polarization has little capability for bending around corners.

Figures 3 and 4 compare results for the unmounted and mounted array. The pattern is symmetrical for the unmounted array with a 50-degree vertical beamwidth at the 3 db point and a front-to-back ratio greater than 25 db. The vertical beamwidth and front-to-back ratio remained the same for the mounted array; however, the beam is no longer symmetrical and is now



NOTES:

1. Frequency 16.2 KMC
2. E Plane 360° Pattern
3. Perpendicular Polarization
4. Wave Guide RG 121/U  
44 Inch Slotted Array  
(Unmounted)

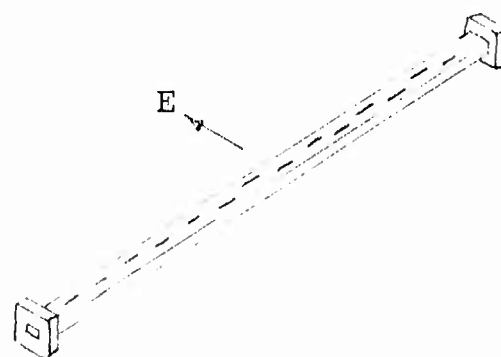
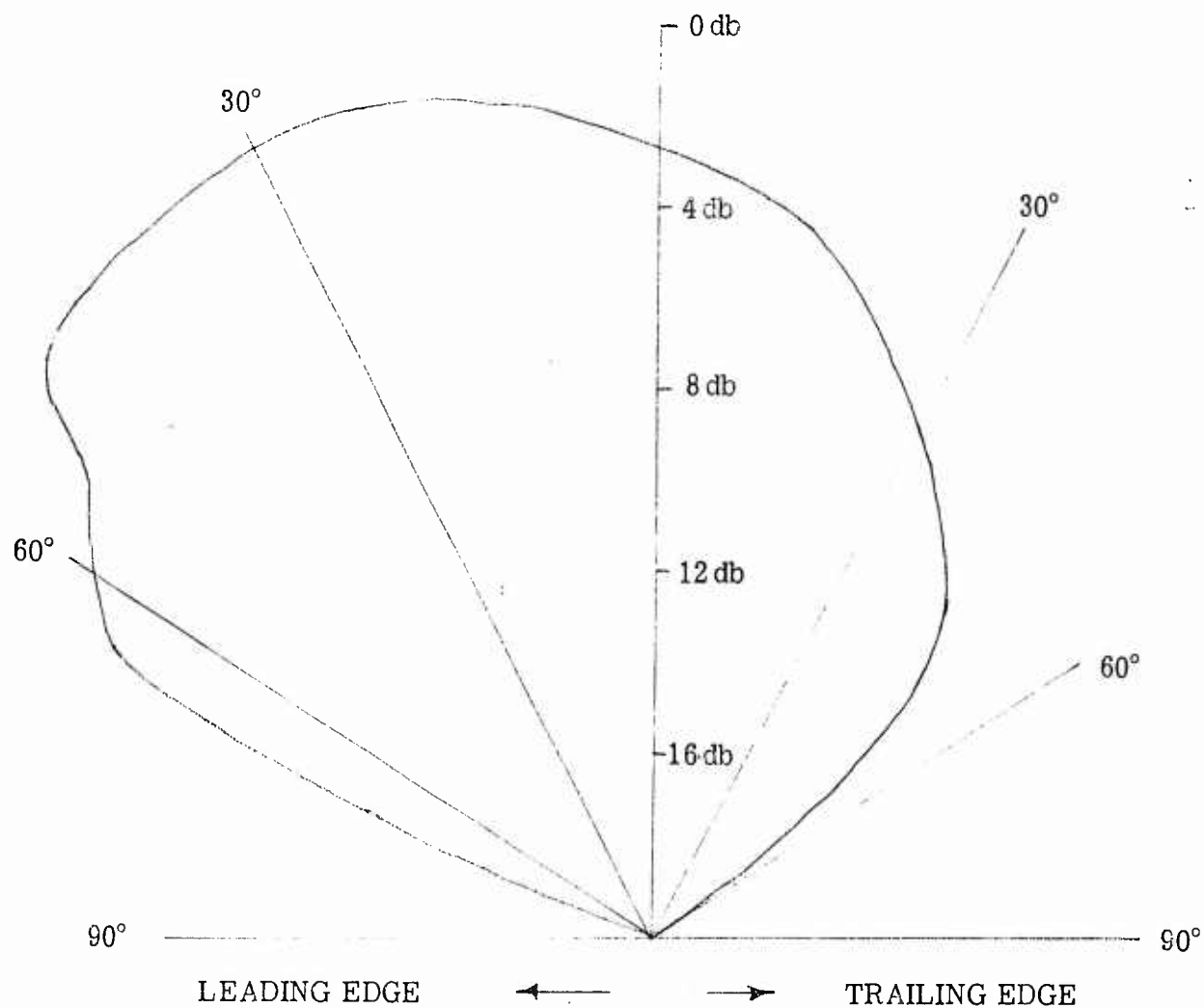


Figure 3. Antenna Pattern for Unmounted Multiple Slot Linear Array



NOTES:

1. Frequency 16.2 KMC
2. E Plane 360° Pattern
3. Perpendicular Polarization
4. Wave Guide RG 121/U  
44 Inch Slotted Array

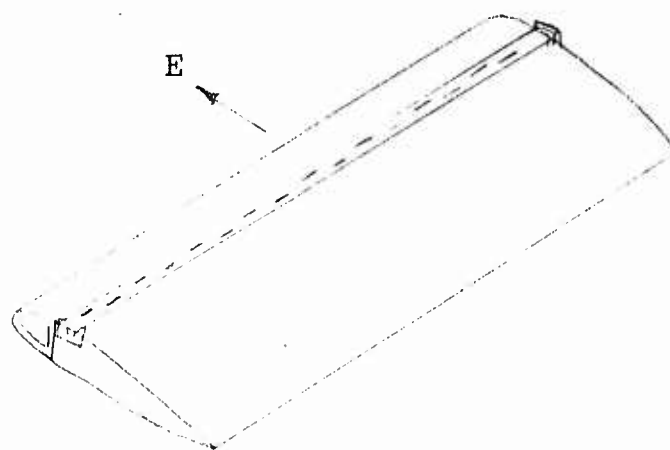
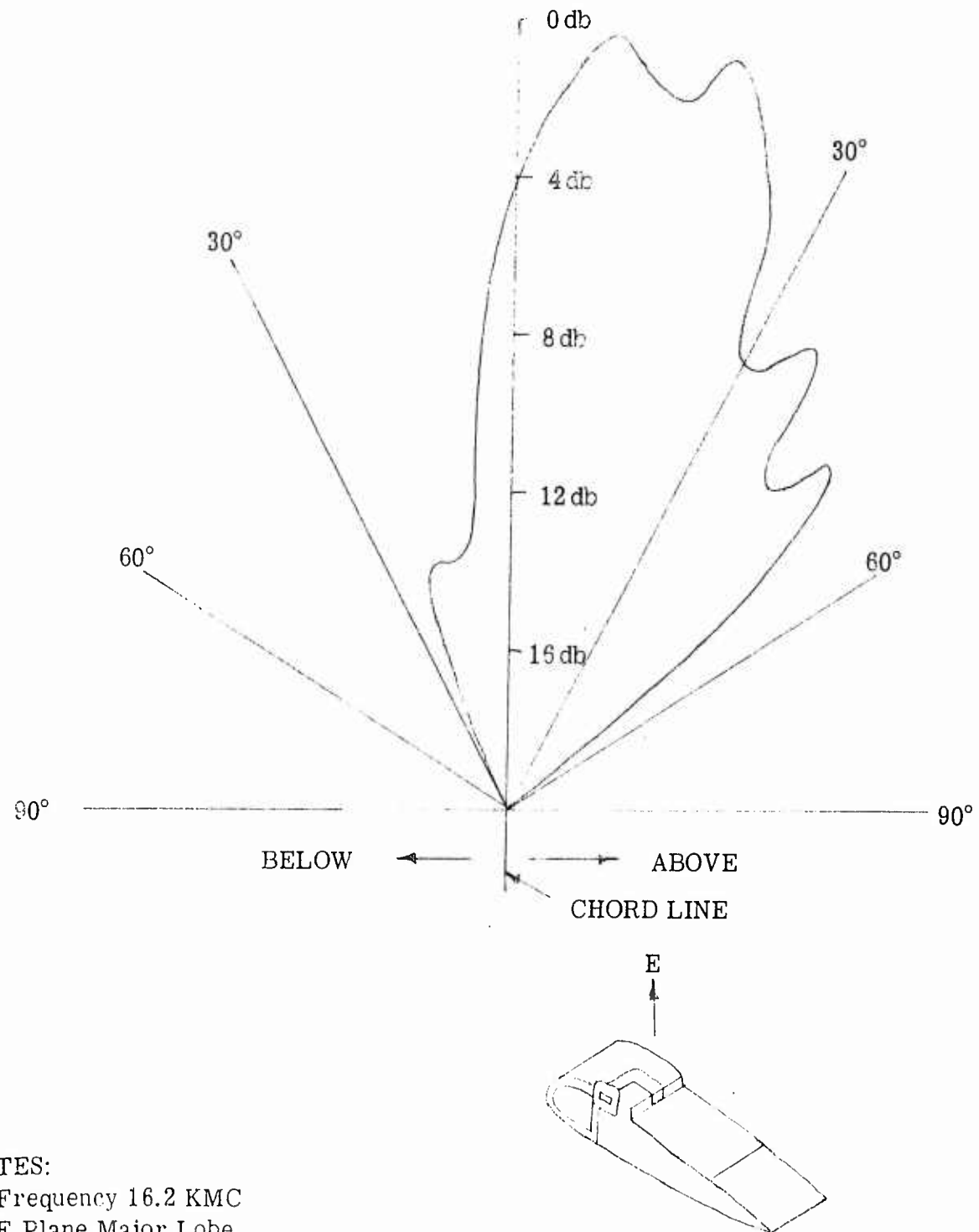


Figure 4. Pattern for Mounted Multiple Slot Linear Array

skewed approximately 25 degrees toward the leading edge.

Figures 5 and 6 show the effect of exposing the honeycomb material. Both patterns are for perpendicular polarization at 16.2 KMC and with RG-91U waveguide. Only the main beams are shown with the front-to-back ratio noted. With the honeycomb exposed the beam has a vertical beamwidth of 12 degrees with one slight reversal occurring in the pattern. Covering the honeycomb gave the same front-to-back ratio, but several reversals occur in the pattern with a beamwidth at the 3 db point of 24 degrees. Both beams are skewed slightly.

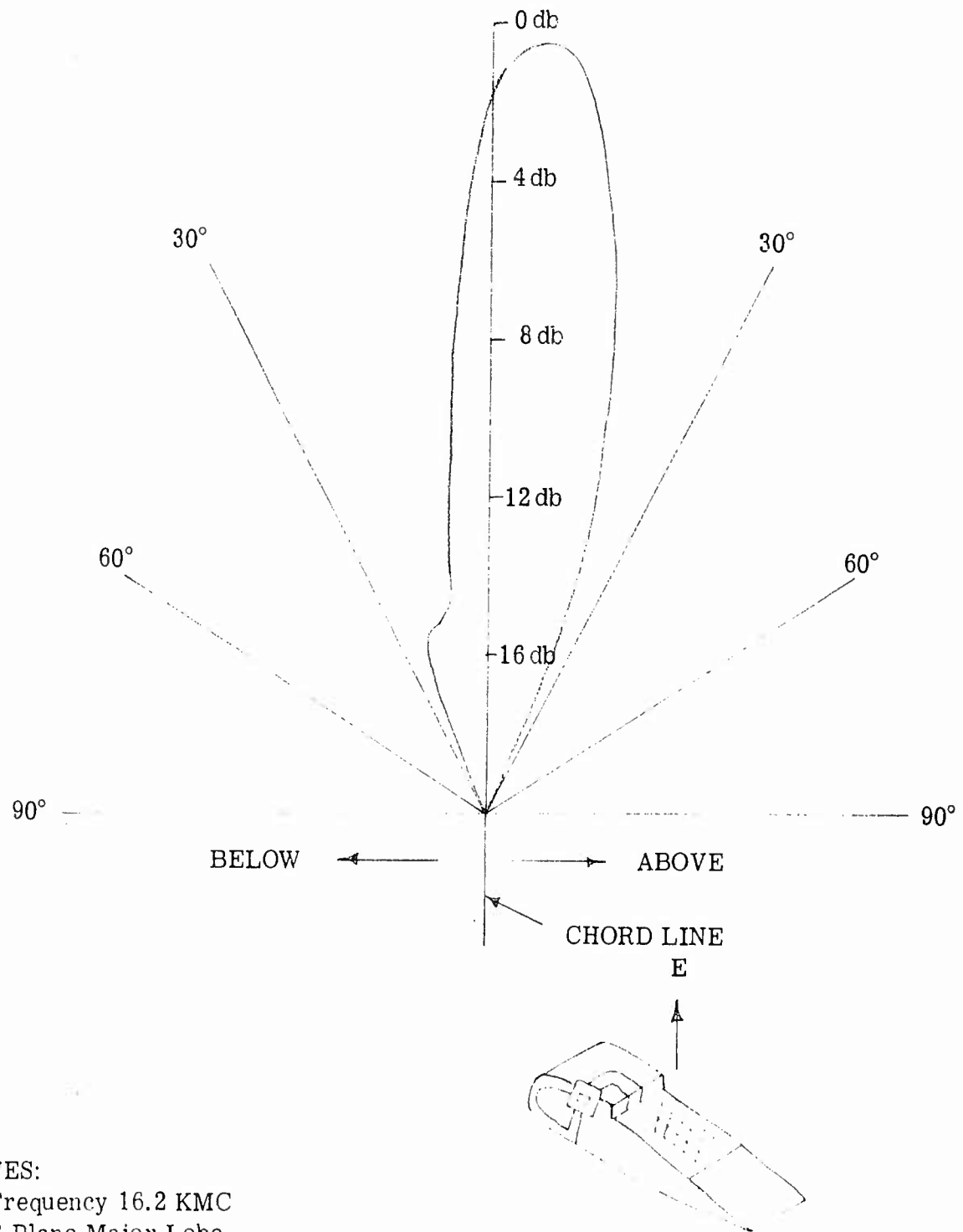
In Figure 7 the slot has been moved close to the trailing edge spar. The beam is again slightly skewed below the chord line of the blade. Front-to-back ratio is considerably better, at 25 db, and the vertical beamwidth is 14 degrees. Reversals in the pattern can again be seen; they are not nearly as severe as in Figure 5. Again only the main beam is shown, but front-to-back ratio noted.



NOTES:

1. Frequency 16.2 KMC
2. E Plane Major Lobe
3. Perpendicular Polarization
4. Wave Guide RG 91/U
5. Cover on Exposed Honey Comb (Cover .001 Aluminum)
6. 15 DB Front to Back Ratio

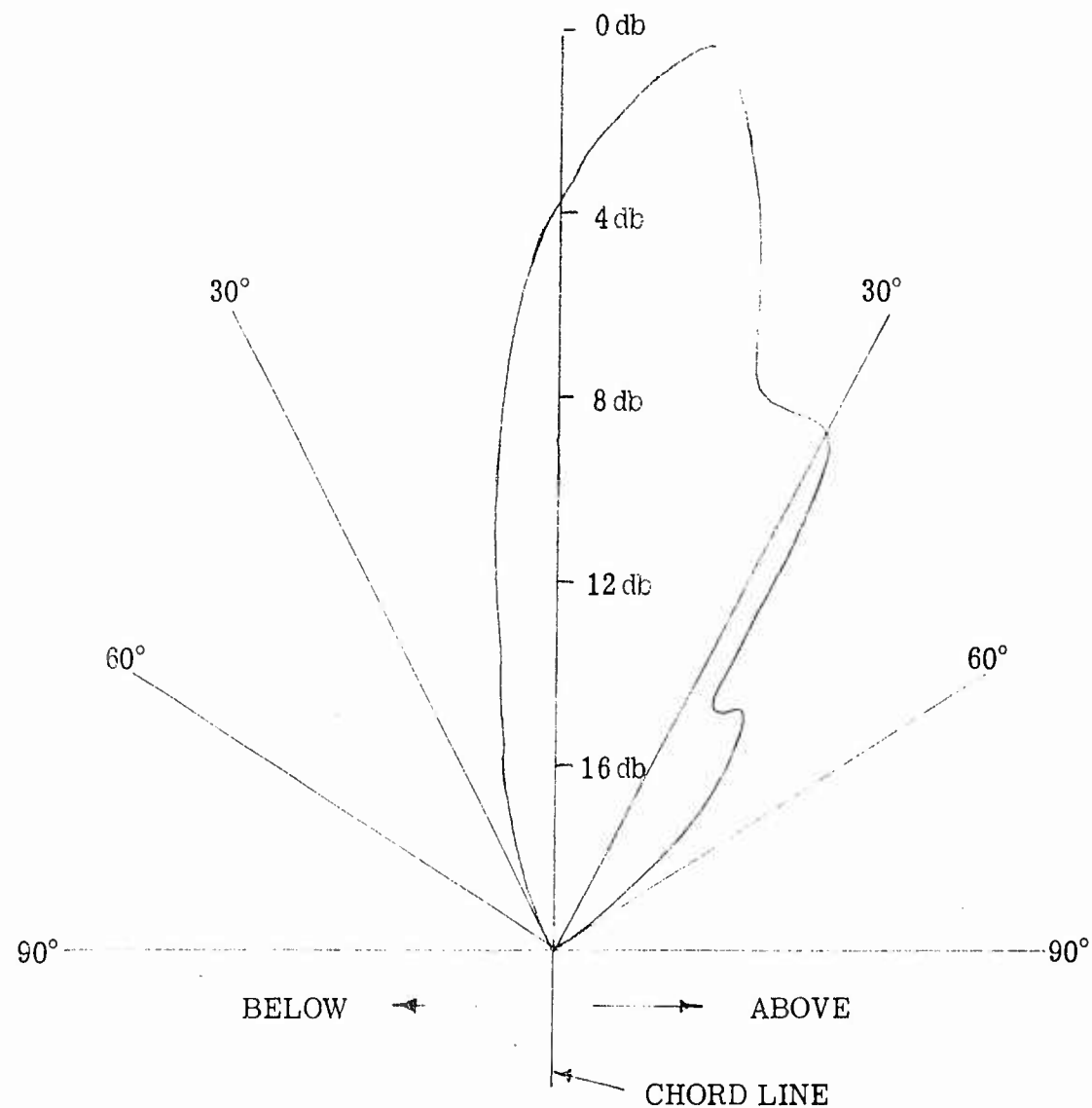
Figure 5. Surface Wave on Long Smooth Surface, Trailing Edge



NOTES:

1. Frequency 16.2 KMC
2. E Plane Major Lobe
3. Perpendicular Polarization
4. Wave Guide RG 91/U
5. Honey Comb Exposed
6. 15DB Front to Back Ratio

Figure 6. Surface Wave on Long Rough Surface Trailing Edge



NOTES:

1. Frequency 16.2 KMC
2. E Plane Major Lobe
3. Perpendicular Polarization
4. Wave Guide RG 91/U
5. 25 DB Front to Back Ratio

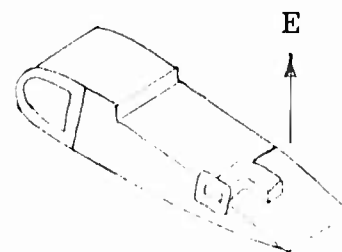


Figure 7. Surface Wave on Short Smooth Surface, Trailing Edge



## B. Single and Dual Slot Blade Sections

### 1. Configurations

Three special blade sections were built and are shown in Figures 9 through 11. A piece of RG-91U waveguide was used to simulate a single slot of an antenna. These sections were used to study the effect of blade geometry on vertical beamwidth and to compare radiation patterns for a single slot and a phased dual slot antenna. Data was also taken on the effect various materials produced on the radar beam. The features of each section were:

1. Section A - Dual slots - to be fed in phase so as to produce a single beam.
2. Section B - Single slot with hetrofoam and the maximum width trailing edge spar (corresponding to the trailing edge from Station 24.5 to Station 60 on the UH-1B blade).
3. Section C - Single slot with cellfoam and the minimum width trailing edge (corresponding to the trailing edge spar from Station 160 to Station 264 on the UH-1B blade).

A sketch of the trailing edge spar is shown in Figure 8. The increase in thickness from tip to root of the blade and the linear taper in the spar from Station 60 to 160 are both shown.

Figure 9 is a photograph of Section A with the hetrofoam and fiberglass removed. Both slots in the blade are identical. The aluminum skin and honeycomb has been milled away and an aluminum "hat" inserted in the groove. The "hat" covers the exposed honeycomb and is flush with the skin of the blade section. The aperture of the slot is positioned as close to the trailing edge as possible consistent with maintaining structural integrity for a full 175-inch blade model. The RG-91U waveguide has

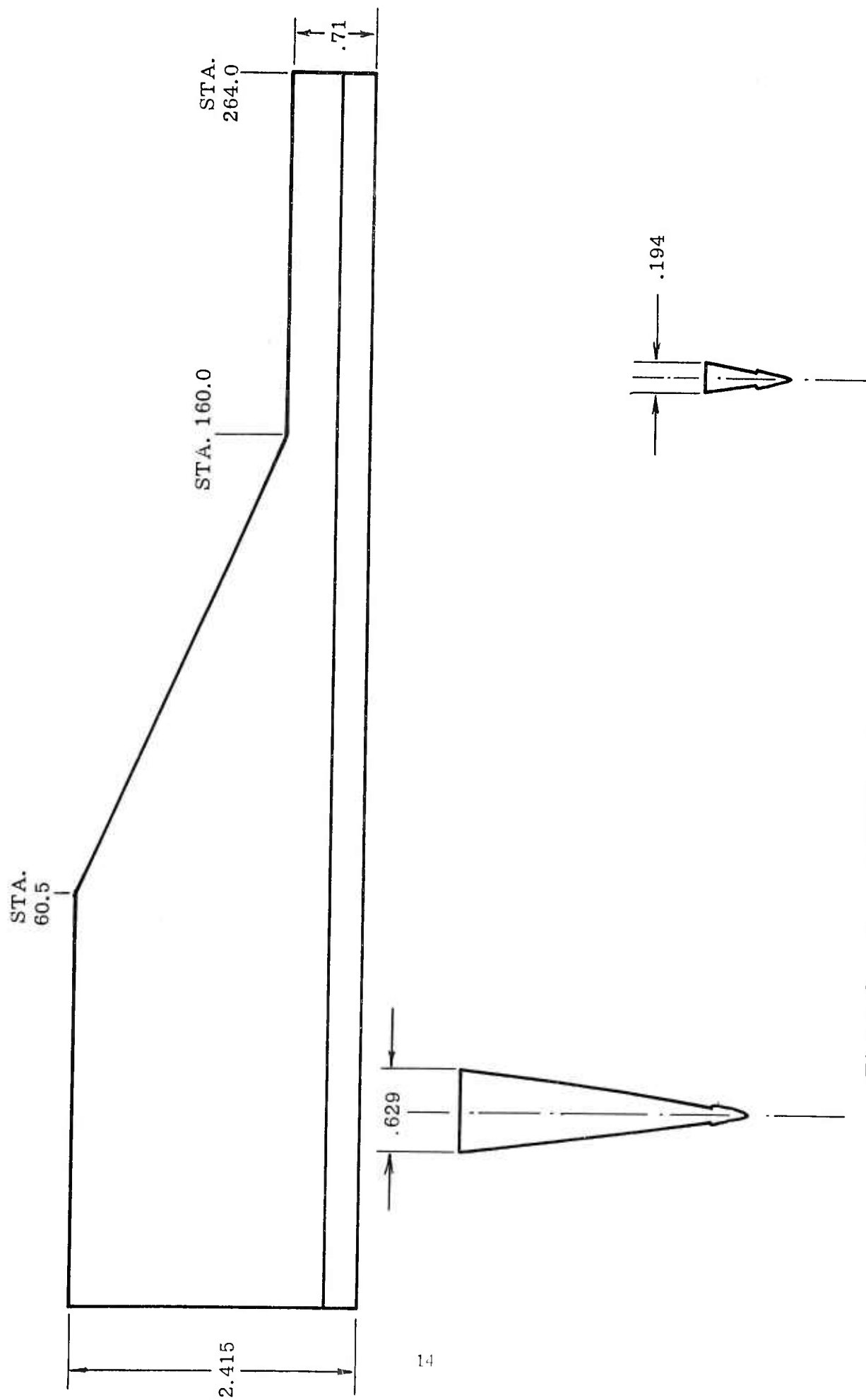


Figure 8. Sketch of Trailing Edge Spar for a UH-1B Rotor Blade

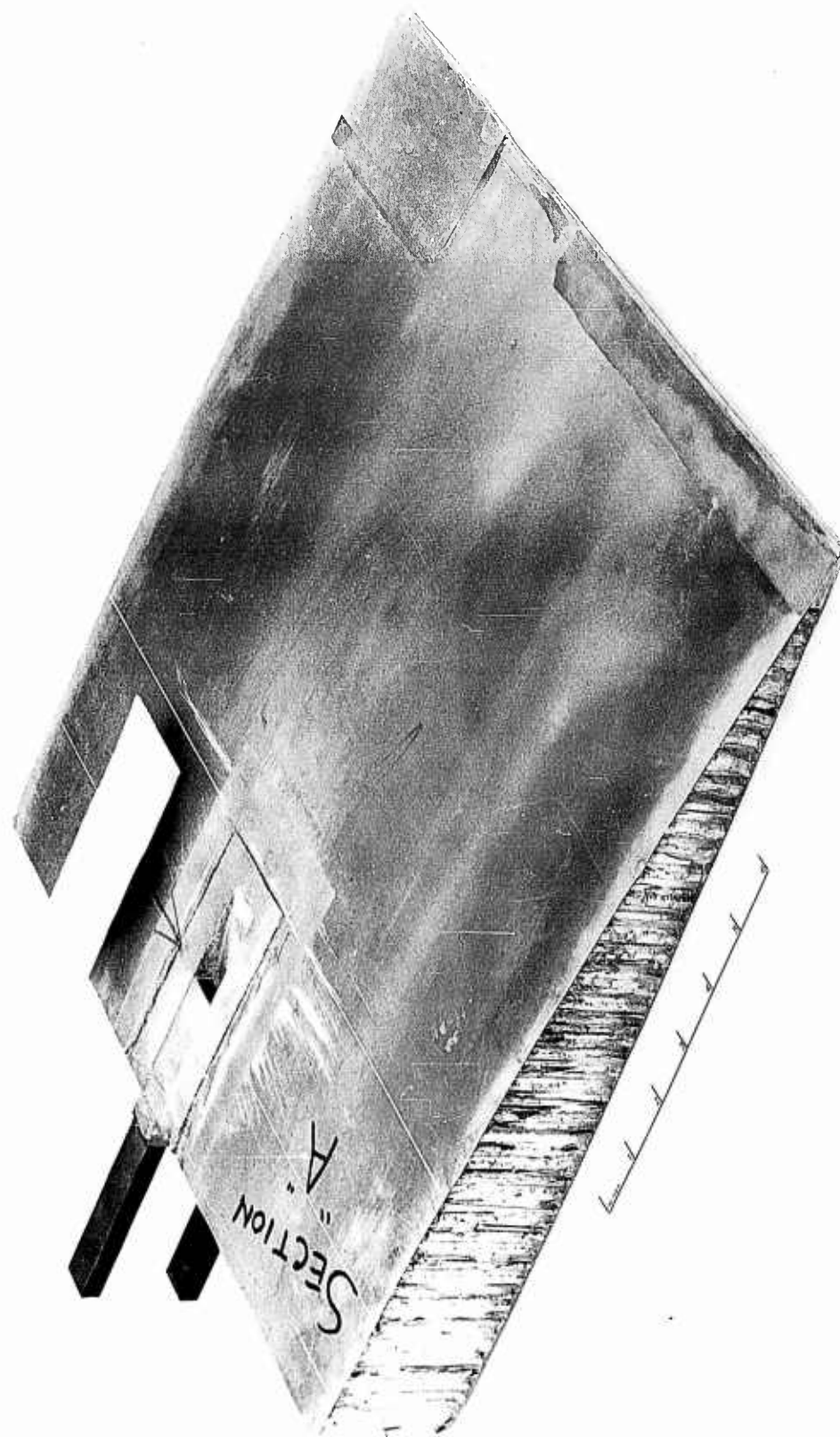


Figure 9. Phased Dual Slot Antenna

been bonded in place parallel with the chord line of the blade. A retro-foam wedge was placed in the hat and a fiberglass skin bonded over the wedge.

Figure 10 and 11 are photographs of Sections B and C. These sections were used to examine the effect of the trailing edge spar on the pattern as well as any effects produced by foams. Both sections were constructed in a similar manner.

The box beam and trailing edge of a section of blade was cut off and a slot cut through the honeycomb material along the chord line of the blade. An aluminum section with a rectangular opening was formed so that the aperture of the waveguide could be positioned precisely along the chord line. The RG-91U guide was then bonded in place.

A section of trailing edge spar was bonded to the solid aluminum wedge. The included angle on the wedge was 30 degrees. Fiberglass skins were bonded to the new trailing edge and wedge assembly. A piece of foam was cut to size and positioned against the wedge. This whole assembly was then bonded to the main blade section with the wedge knife-edge aligned with the center of the waveguide aperture. This positioning was maintained within  $\pm .010$  inches.

## 2. Test Results

The patterns obtained for Section A are shown in Figure 12. Both the individual and the sum pattern are given. Though the sum pattern is quite broad in beamwidth, the lobes at  $\pm 45$  degrees are larger than the central lobe by about 10 db. Improvement in this pattern could be obtained by moving the aperture closer to the trailing edge and milling the groove parallel to the chord line.

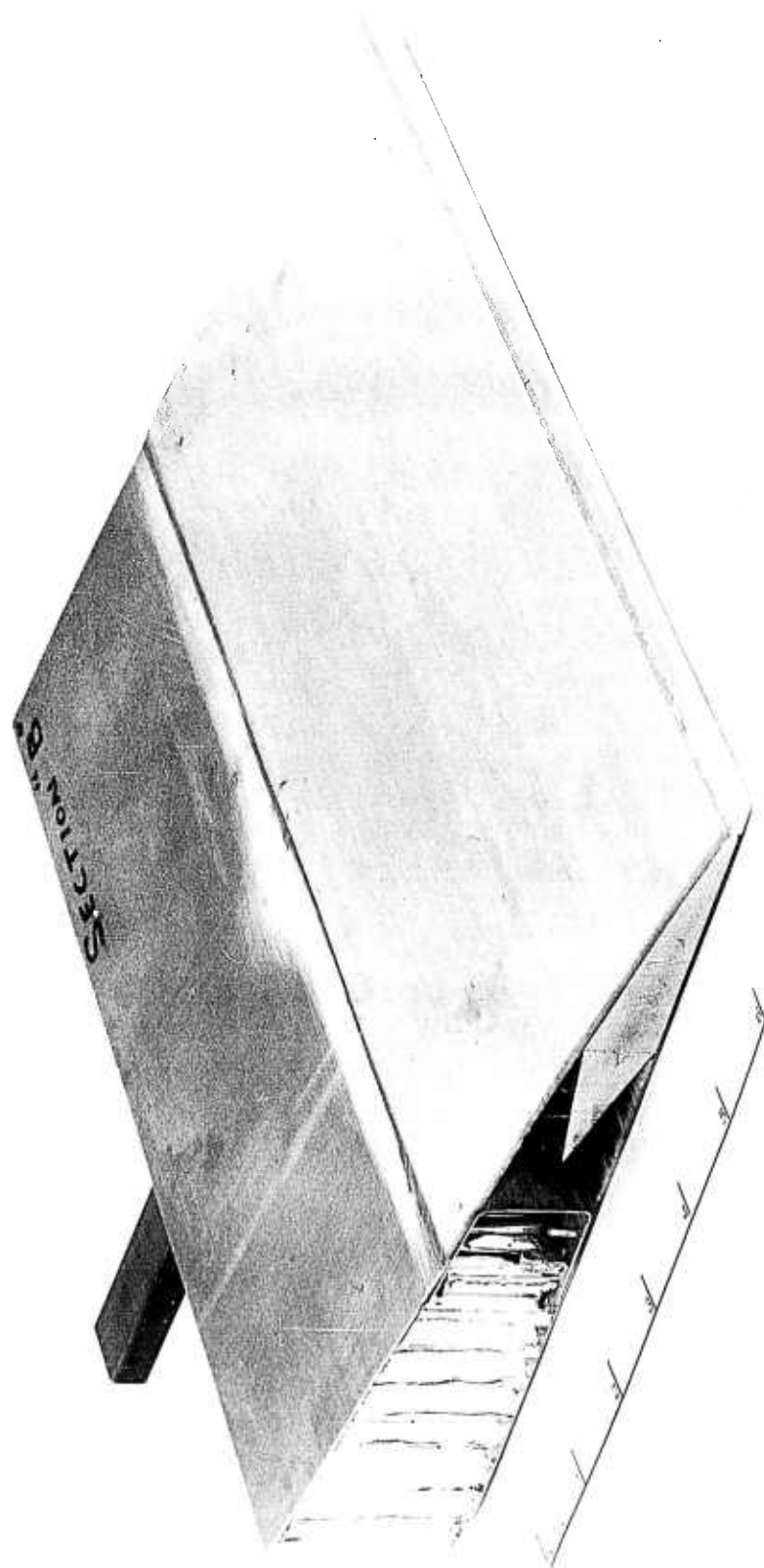


Figure 10. Single Slot Antenna with Maximum Width Trailing Edge

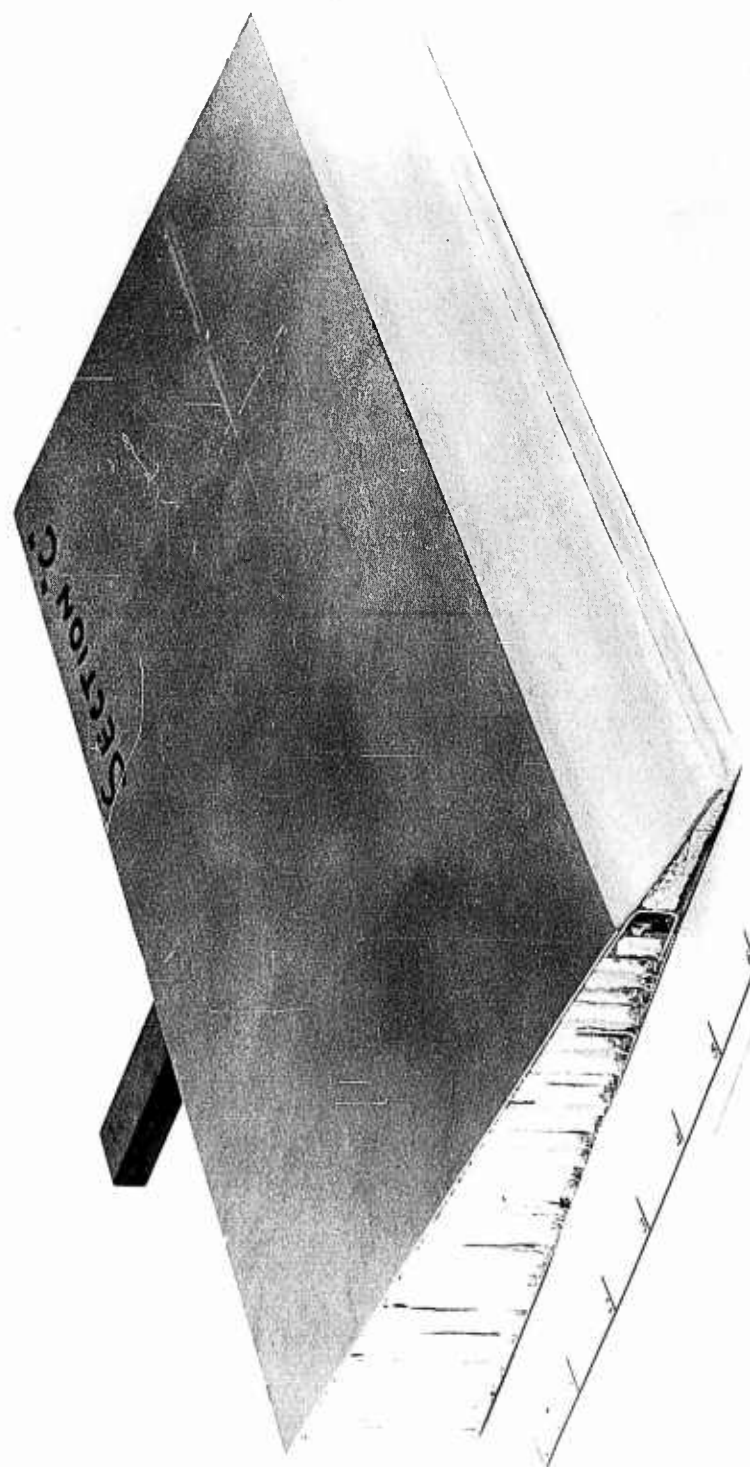


Figure 11. Single Slot Antenna with Minimum Width Trailing Edge

Figures 13 and 14 show vertical patterns for sections B and C. The effect of the thickness of the trailing edge on the vertical pattern is clearly shown. These plots are straight power plots so that the 3 db point is at one half of the vertical scale. The horizontal scale factor on both plots is 10 degrees per centimeter.

The minimum width trailing edge has a vertical beamwidth of 37 degrees at the 3 db point with no significant sidelobes. The maximum thickness trailing edge corresponding to Stations 24.5 to 60 on the UH-1B blade has a beamwidth of 15 degrees with major sidelobes on both sides of the main beam. This is a worst case pattern. The actual section of the blade that would be used if the antenna were placed in the trailing edge would start at Station 91. Here the thickness of the trailing edge is .498 inches as opposed to the .629 inch thickness from Station 60 in to the root. (See Figure 8.)

There are two criteria in selecting any material to be placed between the antenna aperture and free space. The material should be low density and of uniform density. These criteria would apply in our case to both the foam and the fiberglass. Both cellfoam and hetrofoam produced an attenuation of 2 db on the pattern. No phase distortion was detectable.

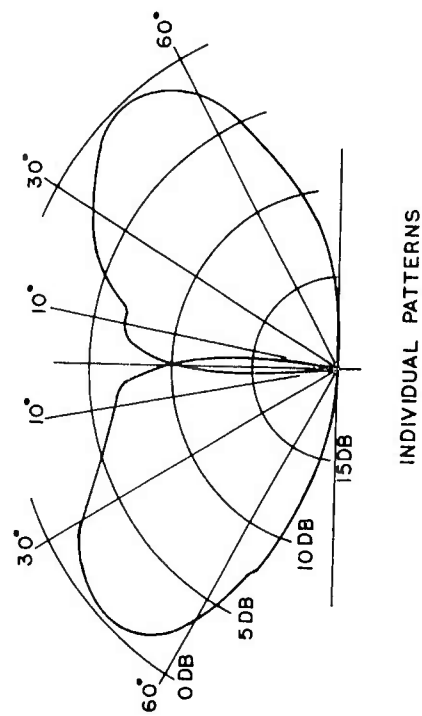
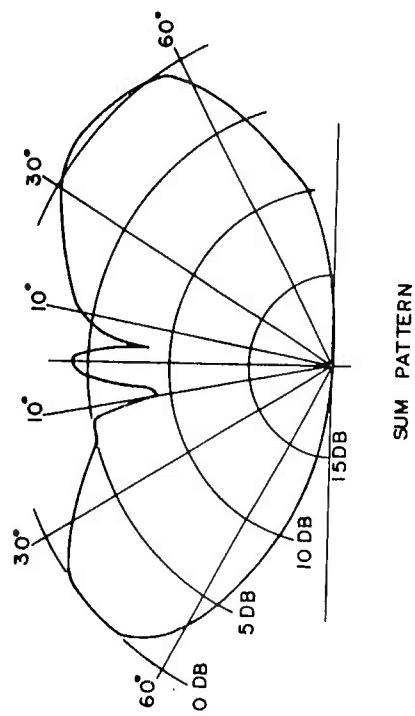


Figure 12. Section A, Elevation Radiation Pattern



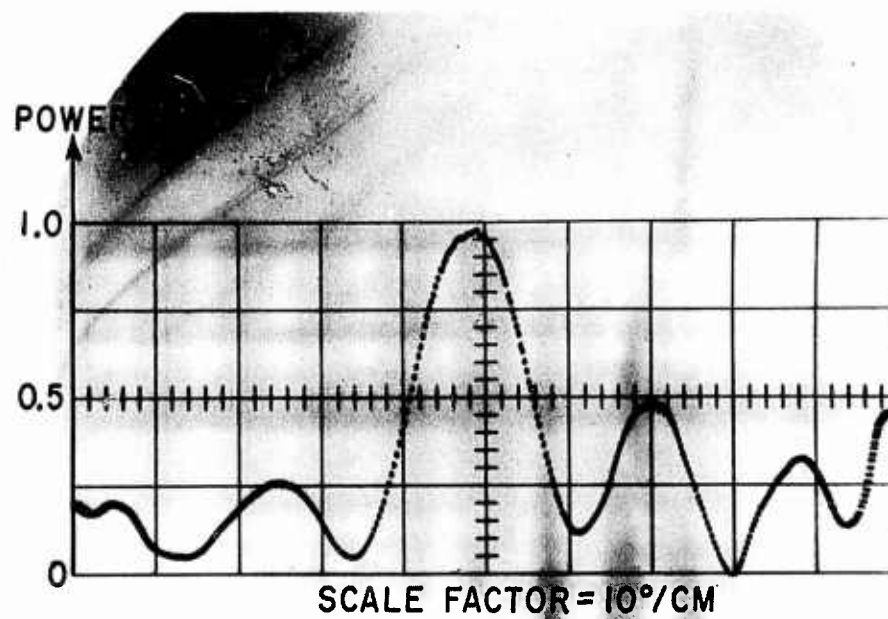


Figure 13 . Vertical Antenna Pattern for Section B

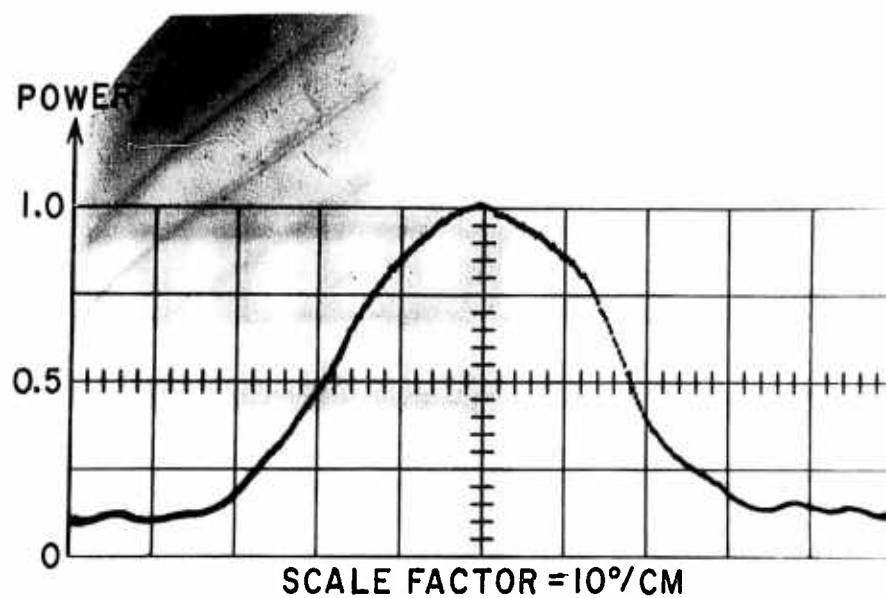


Figure 14 . Vertical Antenna Pattern for Section C

### III. THE TRAILING EDGE BLADE ANTENNA

With the results obtained from the special section tests, the full blade antenna was investigated. Blade geometry and several structural blade modifications were analyzed. A design was selected and a one quarter length model constructed. This 43-inch 60-slot antenna was tested with good results. A 240-slot linear array was designed and tested, and then placed in a 173-inch blade section. The 173-inch 240-slot rotor blade antenna had an azimuth beamwidth of 0.28 degrees with 20 db sidelobes. Vertical beamwidth was 24 degrees and front to back ratio 20 db.

#### A. The 43 Inch 60-Slot Blade Antenna

The 43-inch 60-slot blade antenna shown in Figure 15 was first designed. This configuration was used to check the results of previous tests using an array in the trailing edge of the blade in place of a single slot. The antenna was the one shown in Figure 3 - a 60 slot linear array, end-fed. The section of the blade used was a UH-1B blade from station 140 to 183. Approximately one-half of this blade section has a minimum thickness trailing edge spar. The other half of the spar has a linear taper. An aluminum wedge having an included angle of 30 degrees was bonded to the spar.

##### 1. Configuration

To build this section the trailing edge of the blade ~~was~~ sawed off. The proper section of UH-1B trailing edge spar was selected and the aluminum wedge bonded in place. Fiberglass skins were then attached to the spar to complete the trailing edge assembly. A piece of cellfoam was cut to size and placed in the trailing edge assembly.

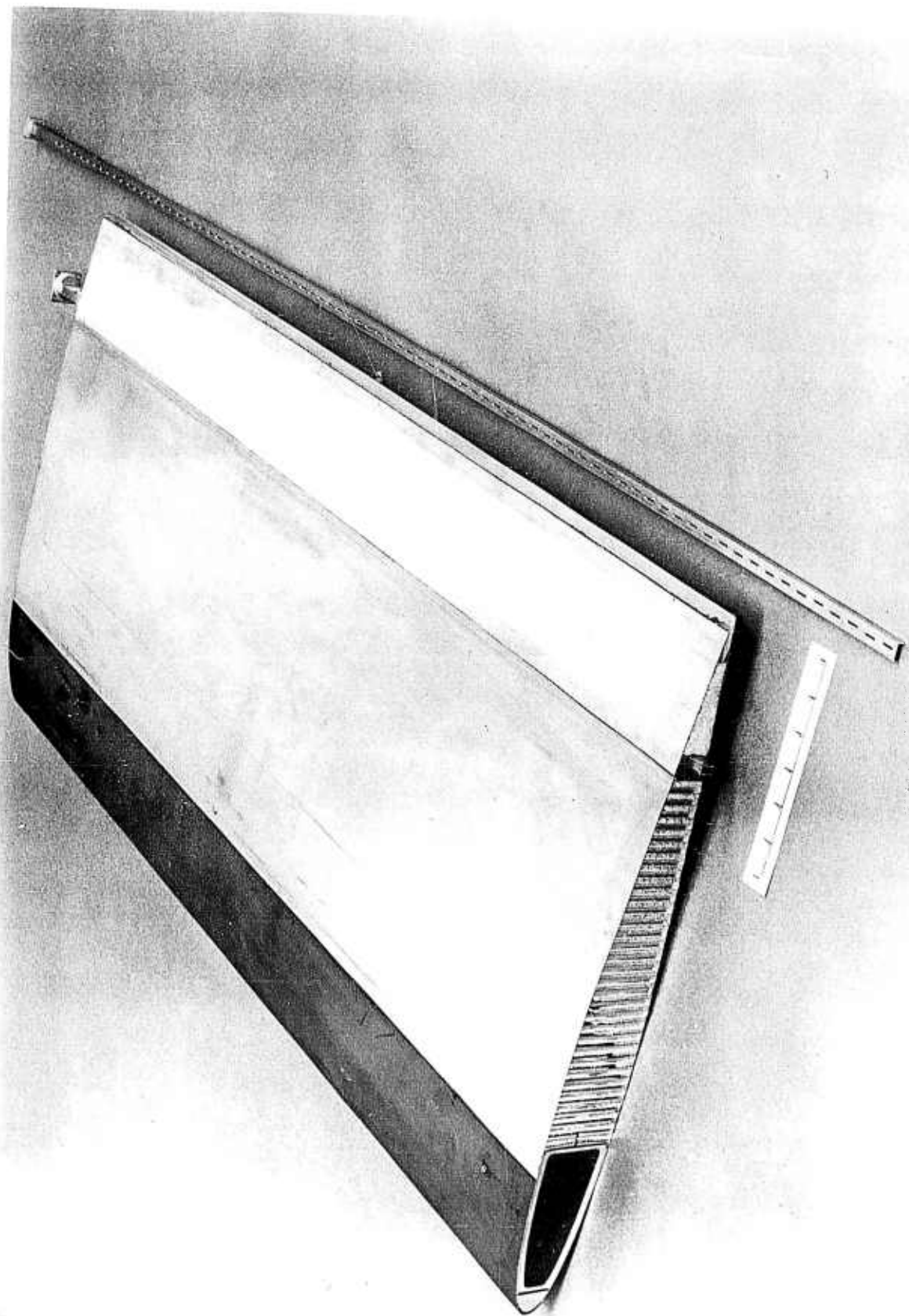


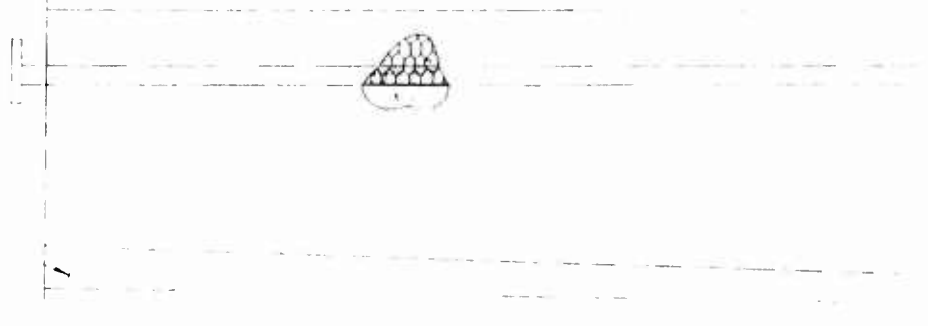
Figure 15. 43 Inch Rotor Blade Section Containing a 60 Slot Linear Array

1



FIL. CLLS. W. 1/2" DP 220  
"C" PROPT. WIDE. 10" V.D.  
BAND GUIDE IN PLACE

A. A. 1. 1/2" 20



2" A. 480 1/2"



3

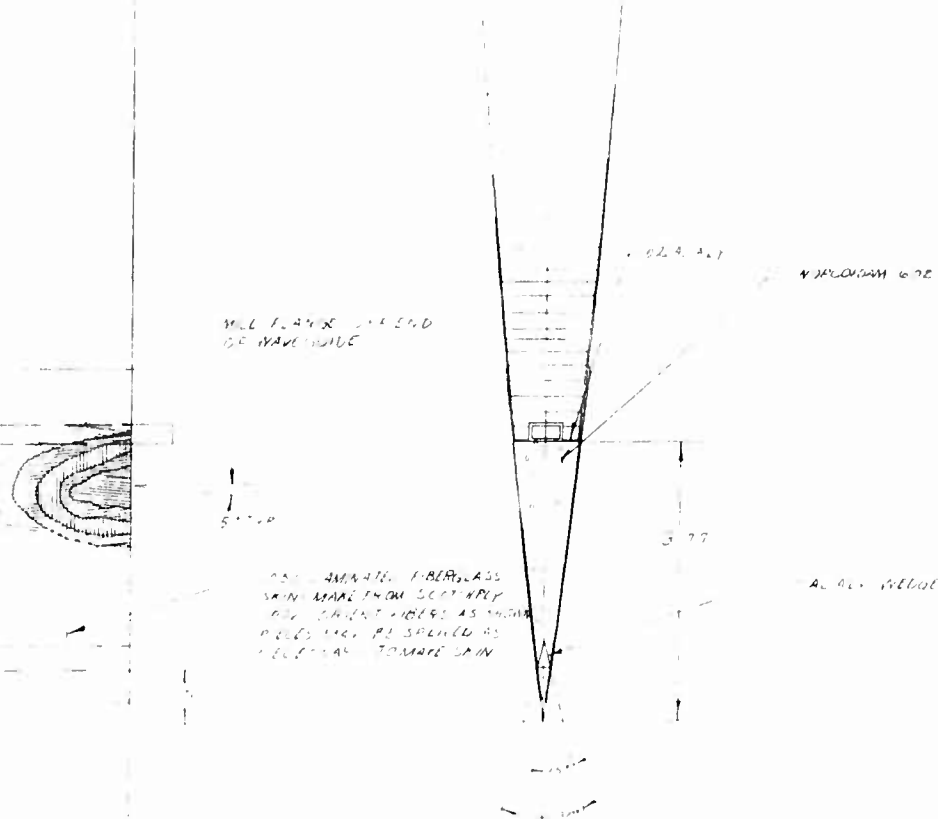


Figure 1C  
Drawing of 43 Inch 60 Slot Trailing Edge Blade Antenna

The forward section of the blade was then prepared. A one-inch deep section of honeycomb was removed from the aft end, which was then replaced with RP-1220, an aluminum filled epoxy. The RP-1220 was milled to a smooth surface. A groove was cut in the RP-1220 for placement of the antenna. The 60-slot array was placed in the groove and the trailing edge assembly then bonded in place. Details of construction are shown in Figure 16.

## 2. Test Results

The blade antenna was tested to determine azimuth beamwidth, sidelobe levels, front to back ratio, and vertical beamwidth. Figures 17 and 18 show the azimuth and vertical beamwidth patterns. Vertical beamwidth is 23 degrees and azimuth beamwidth 1.3 degrees when measured at the Rayleigh range of 50 feet. The sidelobe levels and front to back ratio were both 23 db.

Comparing the results of the blade antenna with the linear array data:

	<u>Array</u>	<u>Blade Antenna</u>
Azimuth Beamwidth	1°	1.35°
Sidelobes	25 db	23 db
Front to back ratio	25 db	23 db
Vertical Beamwidth	50°	24°

Sidelobes and front to back ratio remain approximately identical. The azimuth beamwidth is degraded slightly and the vertical beamwidth considerably. The principle degrading factor is the trailing edge spar assembly. Its thickness decreases vertical beamwidth as was noted in Section IIB. It also produces some phase distortion. For the 43-inch 60 slot blade configuration the trailing edge spar is thicker at one end

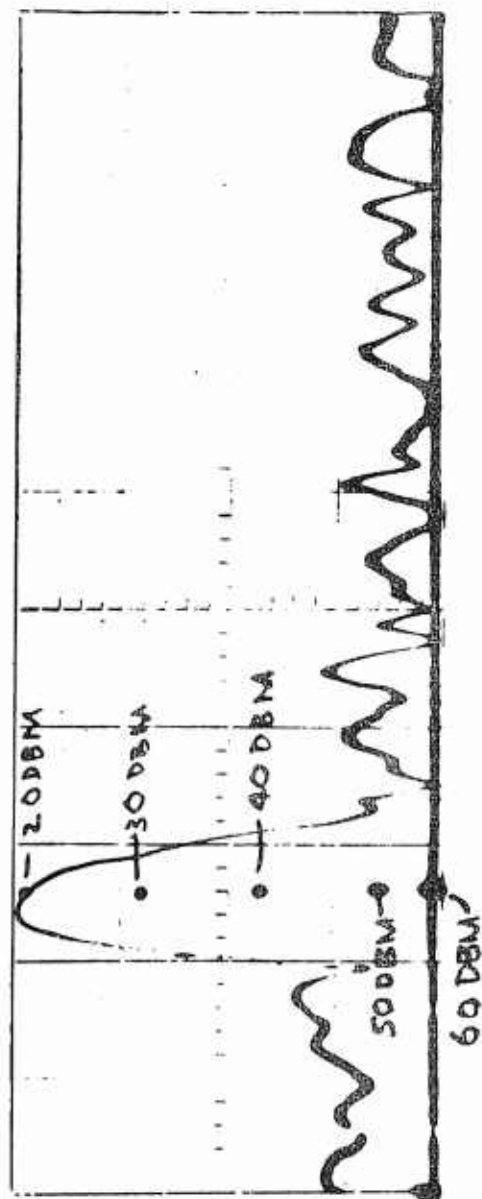


Figure 17. Azimuth Pattern for 43 Inch 60 Slot Trailing Edge Blade Antenna

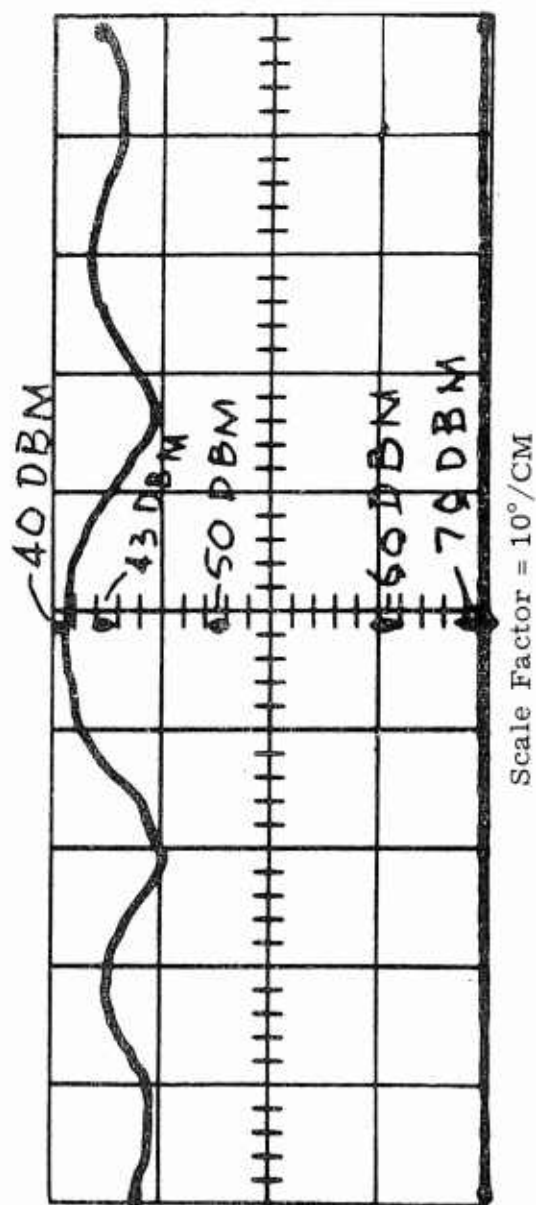


Figure 18. Vertical Pattern for 43 Inch 60 Slot Trailing Edge Blade Antenna



and has a linear taper over only one-half its length. These changes in path length from the antenna aperture to the trailing edge of the blade will tend to produce phase distortion. This phase change modified the antenna pattern, degrading the azimuth beamwidth.

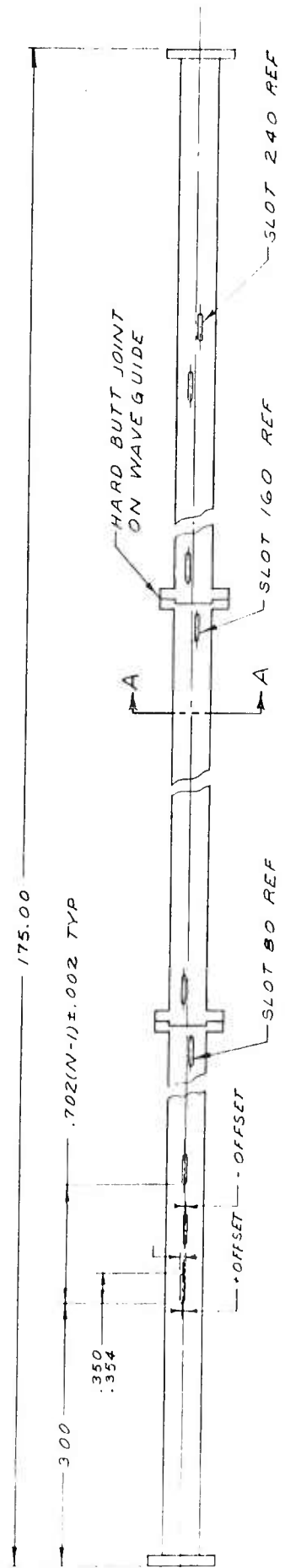
## B. The 240-Slot Array

Fifteen foot slot arrays at 16 to 17 KMC frequencies normally have 400 slots because of one-half wave slot spacing, but by reducing the waveguide size (this is desirable from a structural standpoint) to that having a wavelength twice that of free space, it is possible to have a slot spacing of nearly a wavelength without multiple grating lobes (phase ambiguities). However, even with 240 slots, the cumulative effects of small unexpected changes in the rate of radiation leakage can result in negligible power radiated from one end of the antenna as compared to the other.

The radiation leakage rate or slot conductance is usually determined by testing a few slots covered by various materials acceptable to the antenna designer. The slot conductance in a waveguide is fairly well known; for long antennas it must be adjusted. The total conductance seen by the slot in a rotor blade antenna must take into account the material used in the trailing edge of the blade. The nose antenna design has a similar problem since the waveguide is back a good portion of a wavelength from the leading edge, requiring small transmission lines from the waveguide to the leading edge of the blade (see Section V).

### 1. Configuration

The array was designed using results reported by T. T. Taylor and Andre Dion (see references). The waveguide used was K<sub>7</sub> (0.5 x 0.25 inches outside dimension). A 30 db sidelobe criterion was used with 5% power to the load at a frequency of 16.15 KMC. Figure 19 shows the array layout together with slot size, slot spacing, and slot tolerance. Table 1 gives the offset distances for the array and a plot of these distances is shown in Figure 20 without regard to sign. Table 1 notes that adjacent slots



NOTE:  
1. TOLERANCE ON OFFSET FROM Q.  
SLOT 1 THRU 50 ± .001  
SLOT 51 THRU 240 ± .002  
2. MATERIAL:  
WAVEGUIDE - RG121/U 1100 AL ALY  
FLANGES - UG-597/U (2 STANDARD, 4 MODIFIED)

Figure 19. The Slotted Array

TABLE 1

Slot Offset Distances for a Taylor Power Distribution  
 With 30 db Sidelobes and 5% Power to the Load at Frequency of 16.15 KMC

Slot No.	Slot Offset	Slot No.	Slot Offset
1	+.011	44	-.023
2	-.011	45	+.024
3	+.011	46	-.024
4	-.011	47	+.025
5	+.011	48	-.025
6	-.011	49	+.026
7	+.011	50	-.026
8	-.011	51	+.027
9	+.012	52	-.027
10	-.012	53	+.028
11	+.012	54	-.028
12	-.012	55	+.029
13	+.012	56	-.029
14	-.012	57	+.030
15	+.012	58	-.030
16	-.013	59	+.031
17	+.013	60	-.031
18	-.013	61	+.032
19	+.013	62	-.032
20	-.014	63	+.033
21	+.014	64	-.034
22	-.014	65	+.034
23	+.014	66	-.035
24	-.015	67	+.035
25	+.015	68	-.036
26	-.015	69	+.036
27	+.016	70	-.037
28	-.016	71	+.037
29	+.016	72	-.038
30	-.017	73	+.039
31	+.017	74	-.039
32	-.018	75	+.040
33	+.018	76	-.040
34	-.018	77	+.041
35	+.019	78	-.041
36	-.019	79	+.042
37	+.020	80	-.042
38	-.020	81	+.043
39	+.021	82	-.044
40	-.021	83	+.044
41	+.022	84	-.045
42	-.022	85	+.045
43	+.023	86	-.046

TABLE 1 (Cont'd)

<u>Slot No.</u>	<u>Slot Offset</u>	<u>Slot No.</u>	<u>Slot Offset</u>
87	+.046	134	-.073
88	-.047	135	+.074
89	+.048	136	-.074
90	-.048	137	+.075
91	+.049	138	-.075
92	-.049	139	+.076
93	+.050	140	-.076
94	-.050	141	+.077
95	+.051	142	-.077
96	-.052	143	+.078
97	+.052	144	-.078
98	-.053	145	+.079
99	+.053	146	-.079
100	-.054	147	+.080
101	+.054	148	-.080
102	-.055	149	+.081
103	+.056	150	-.081
104	-.056	151	+.081
105	+.057	152	-.082
106	-.057	153	+.082
107	+.058	154	-.083
108	-.058	155	+.083
109	+.059	156	-.083
110	-.060	157	+.084
111	+.060	158	-.084
112	-.061	159	+.085
113	+.061	160	-.085
114	-.062	161	+.085
115	+.063	162	-.086
116	-.063	163	+.086
117	+.064	164	-.086
118	-.064	165	+.087
119	+.065	166	-.087
120	-.065	167	+.087
121	+.066	168	-.087
122	-.066	169	+.088
123	+.067	170	-.088
124	-.068	171	+.088
125	+.068	172	-.088
126	-.069	173	+.088
127	+.069	174	-.088
128	-.070	175	+.088
129	+.070	176	-.088
130	-.071	177	+.088
131	+.071	178	-.088
132	-.072	179	+.088
133	+.072	180	-.088

TABLE 1 (Cont'd)

<u>Slot No.</u>	<u>Slot Offset</u>	<u>Slot No.</u>	<u>Slot Offset</u>
181	+.088	212	-.067
182	-.088	213	+.066
183	+.088	214	-.065
184	-.087	215	+.064
185	+.087	216	-.063
186	-.087	217	+.062
187	+.086	218	-.061
188	-.086	219	+.060
189	+.085	220	-.059
190	-.085	221	+.059
191	+.084	222	-.058
192	-.084	223	+.057
193	+.083	224	-.056
194	-.082	225	+.056
195	+.082	226	-.055
196	-.081	227	+.055
197	+.081	228	-.054
198	-.080	229	+.054
199	+.079	230	-.053
200	-.078	231	+.053
201	+.077	232	-.052
202	-.076	233	+.052
203	+.075	234	-.052
204	-.074	235	+.052
205	+.074	236	-.052
206	-.072	237	+.052
207	+.072	238	-.052
208	-.070	239	+.052
209	+.070	240	-.052
210	-.069	241	+.052
211	+.068		

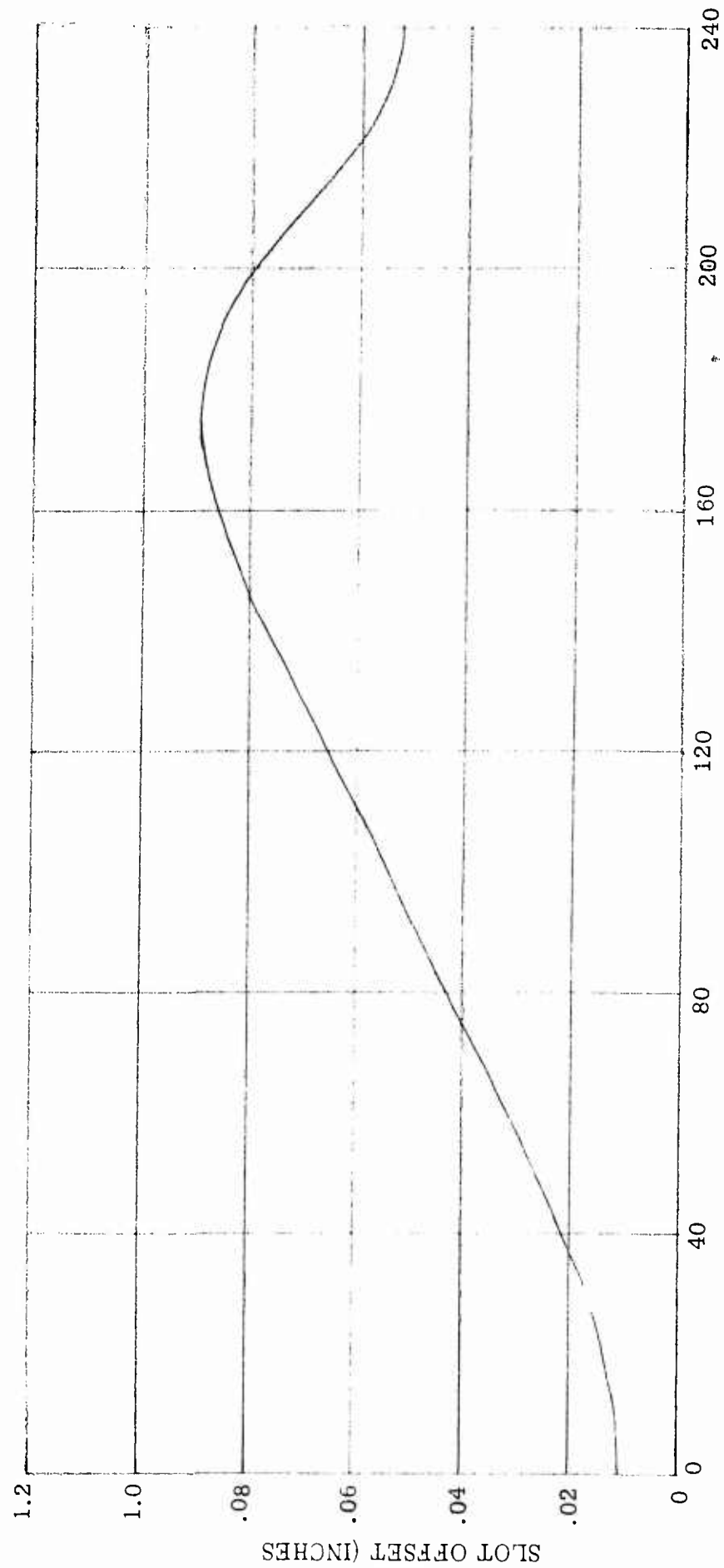


Figure 20. Slot Offset Distances at 16.15 KMC for 30 db Side Lobes and 5% Power to the Load

are on opposite sides of the centerline of the waveguide for phasing purposes.

## 2. Test Results

The 175-inch 240-slot array was mounted on a fixture to hold it straight, and then taken to the Sepulveda basin area in Los Angeles County for testing. This location was used because of its large unobstructed area. An unobstructed 360 degree field of view is a requirement for side-lobe and front-to-back ratio measurement when testing such a large aperture antenna. Figure 21 shows the measured azimuth pattern. The azimuth beamwidth was 0.33 degrees at the 3 db point when measured at the Rayleigh Range of 1600 feet. Sidelobe levels were 23 db with a front-to-back ratio of 23 db.



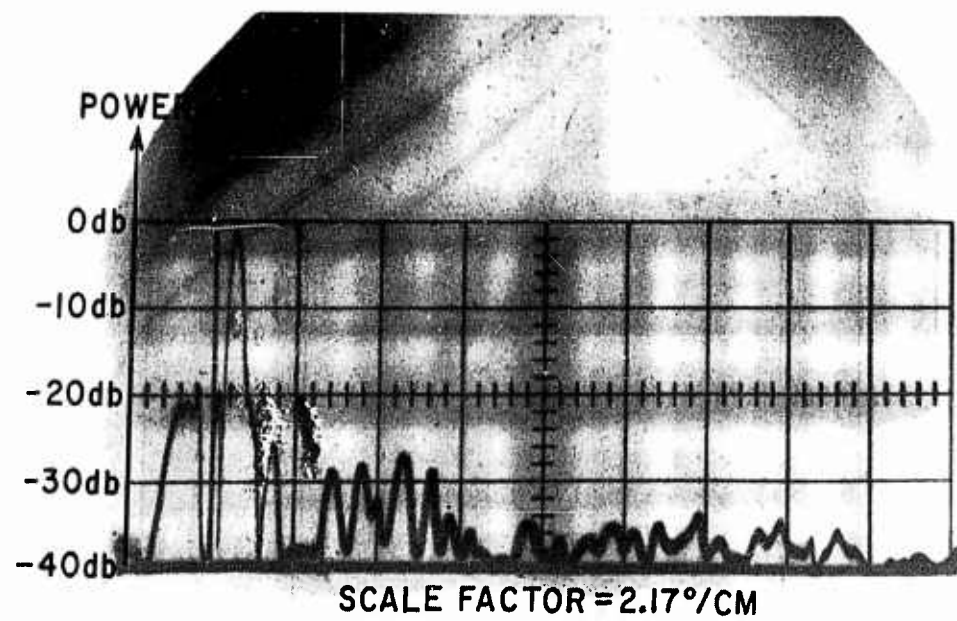


Figure 21. Azimuth Pattern for 240 Slot Array

### C. The 173-Inch 240-Slot Blade Antennas

A 173-inch 240-slot Ku band antenna must produce a smooth, tapered, symmetrical power distribution with a uniform phase front if a good balance between beamwidth and sidelobe levels is to be achieved. Power distribution is the most difficult parameter to control, except in the region of the trailing edge where the geometry of the blade varies along the length of the antenna.

The amount of energy coupled from the waveguide to free space is critical. If many of the slots nearest the transmitter radiate more power than expected, there will be very little radiation from the other end of the antenna, resulting in an asymmetrical power distribution. The amount of power radiated from a slot compared to the power in the guide available to that slot is well known. However, the environment surrounding the slot must be considered in evaluating the radiated power. If the environment along the array varies, compensation must be incorporated into the design.

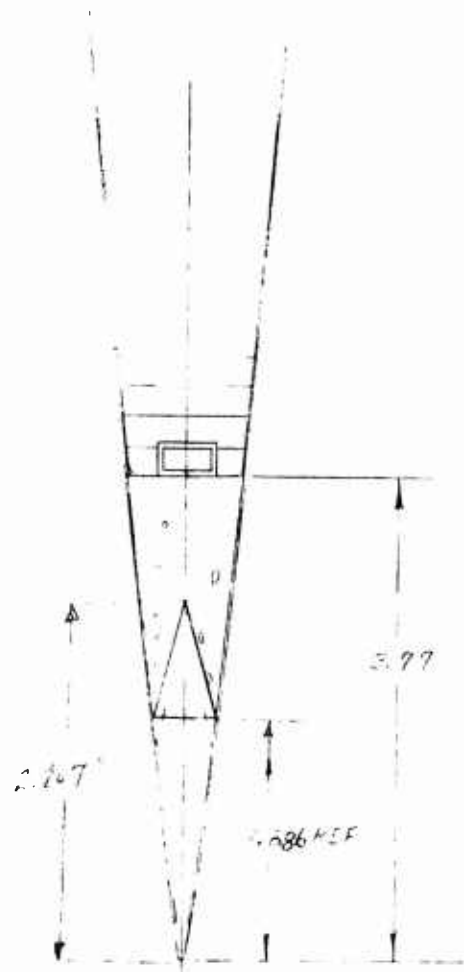
#### 1. Configuration

Figure 22 is a drawing of the 173-inch blade antenna section. A scrap UH-1B rotor blade was secured and the inboard 66.5 inches sawed off. Only the outboard section was used. The trailing edge of the section was first sawed off. About one inch of honeycomb material was removed from the nose section and RP-1220 packed in its place. After hardening, the RP-1220 was milled to a smooth surface with a groove for holding the antenna in the center. A "hat" was formed using 1 mil aluminum foil and both the "hat" and the array inserted into the groove.

Fiberglas skins (.050 inches thick) were bonded to the trailing edge spar, to which the wedge had also been bonded. Cellfoam was cut to fill the space between the array and the trailing edge wedge. The pieces were then assembled.

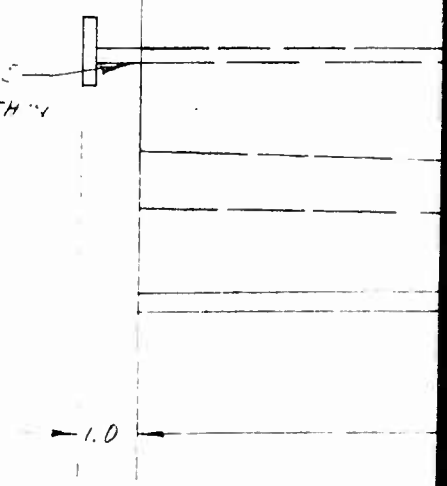
ST1  
310

1



STATION 91

THIS EDGE OF LENS  
TO BE STRAIGHT WITHIN  
.01



371  
210

2

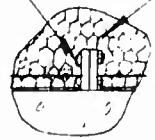
301  
302

1.0

69.0 REF

3

#2 SCREEN NOT  
3 RECS



END OF  
TAPER

HALF SCALE

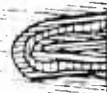
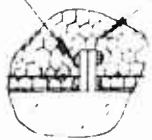
STATION  
160

4

STA  
264.0

REMOVE CORE TO CLEAR SPLINE  
FILL CELLS WITH RP1220 TO SUPPORT WAVEGUIDE

12 BUSHING  
3 R102



5" TYP

1000  
2411  
1002  
5104

STA  
264.0

5

LINE  
TO SUPPORT WAVEGUIDE

5" TYP

.050 FIBERGLASS SAND-  
LAMINATE FROM SCOTCH-PLY  
100% ORIENT FIBERS AS  
SHOWN

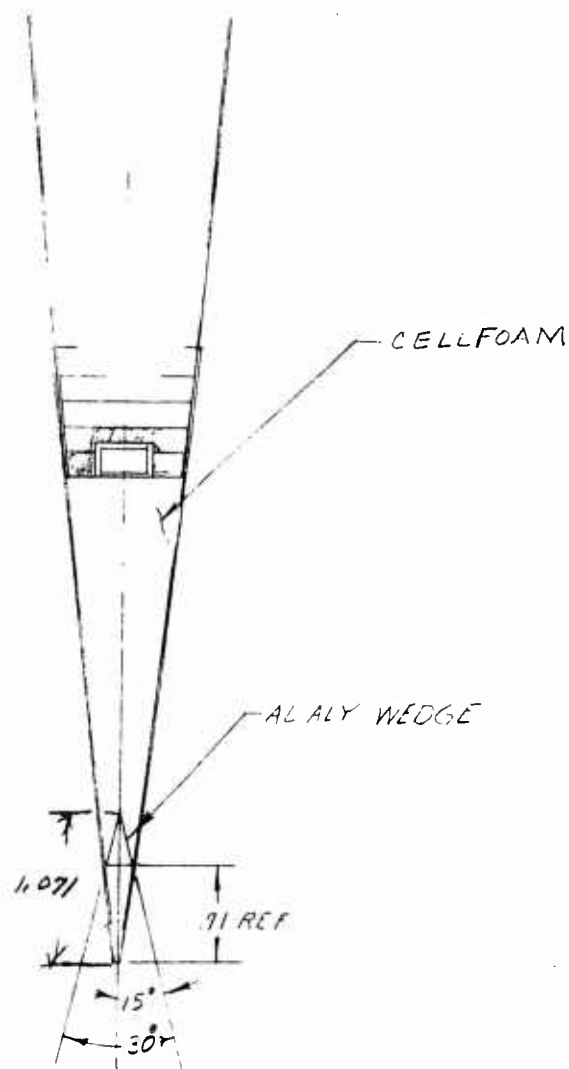


Figure 22  
Drawing of 173 Inch 240 Slot Blade Antenna

Figure 23 shows the nose section, one-third of the array, and the trailing edge sections of the blade. In Figure 24 the array section has been placed in the groove. The 1 mil aluminum foil "hat" is not shown. Note that the slots in the array have been covered by a thin piece of fiberglass for protection.

In Figure 25 the pieces are shown assembled. The cellfoam has been left out for clarity so that the array and trailing edge sections could be seen.

The cellfoam was positioned in the trailing edge section. The three sections of the array were fastened together and, together with the "hat", placed in the groove. The trailing edge assembly was then positioned and the blade antenna placed in a UH-1B bonding tool. The blade section was then covered with a vacuum bag and bonded at room temperature under a pressure of 10 psi. The shape of the tool applied the twist common to all UH-1B blades.

## 2. Test Results

The first test of the blade antenna was at 16.35 KMC. Reasonable beamwidth was obtained; however, a 12 db sidelobe (one-sided) was present in the pattern. The frequency was adjusted to see if the 12 db sidelobe could be suppressed at the expense of the sidelobe on the other side of the beam, in an attempt to achieve sidelobe balance. At 15.98 KMC the pattern was satisfactory. Pictures were taken of the oscilloscope traces and the field test facility dismantled.

In examining the pictures under a magnifying glass the following day, it was discovered that the azimuth beamwidth was 0.6 degrees. A power distribution measurement was then made on the antenna in the laboratory. The power distribution was symmetrical at 15.98 KMC, but power was distributed





Figure 23. Pieces of 173 Inch Blade Antenna Ready for Assembly

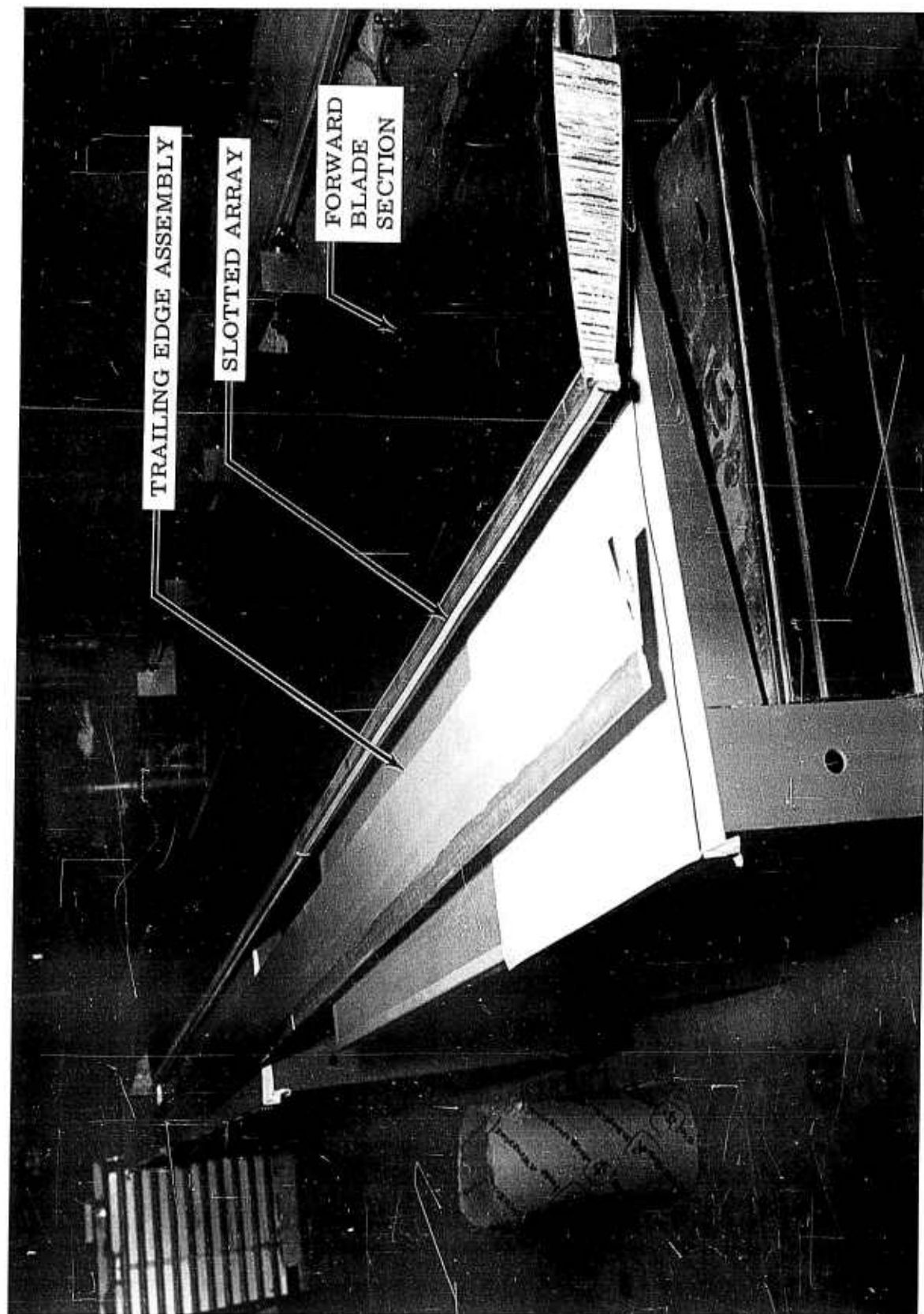


Figure 24. 173 Inch Blade Section With 1/3 of the Slotted Array in the Groove

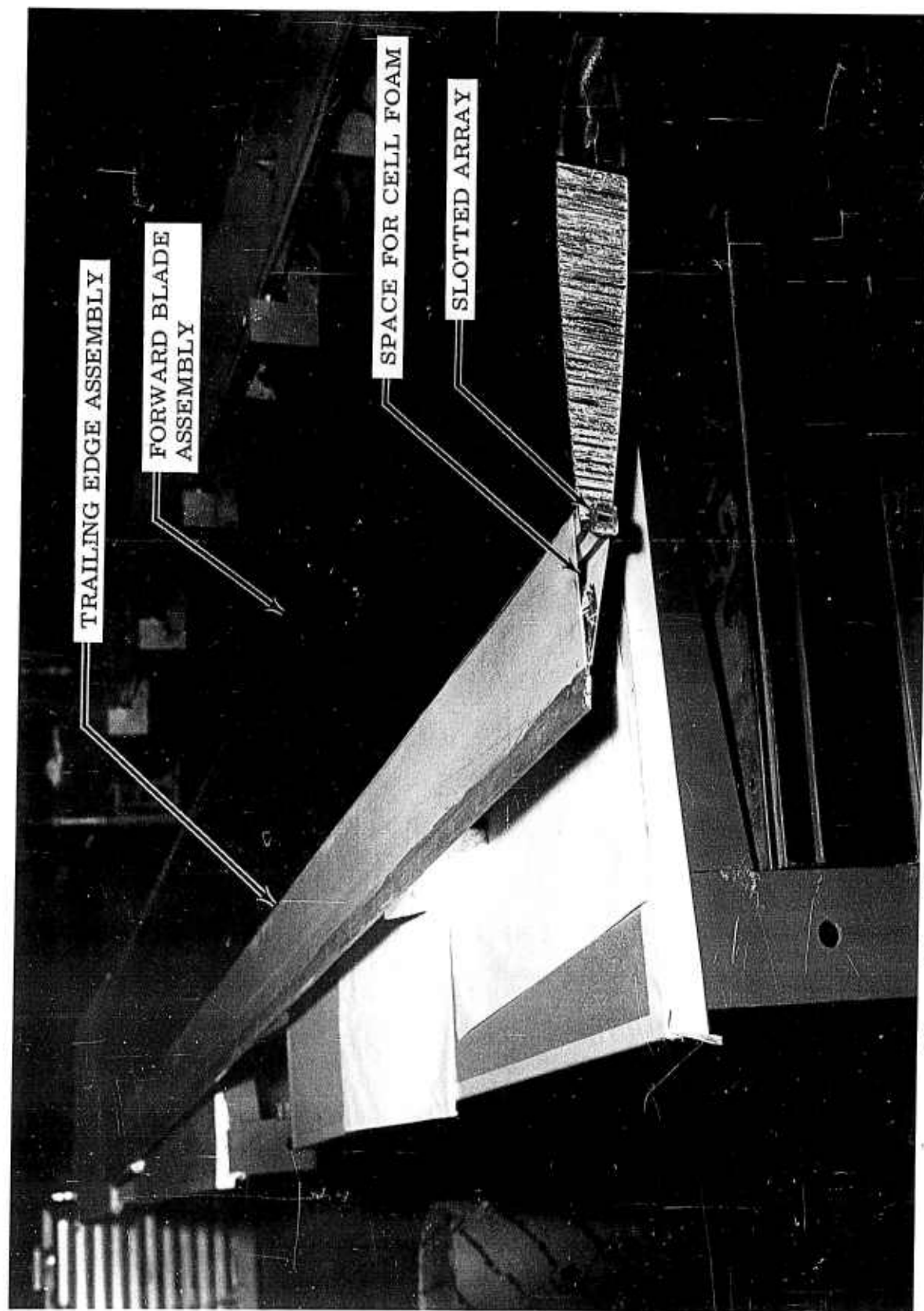


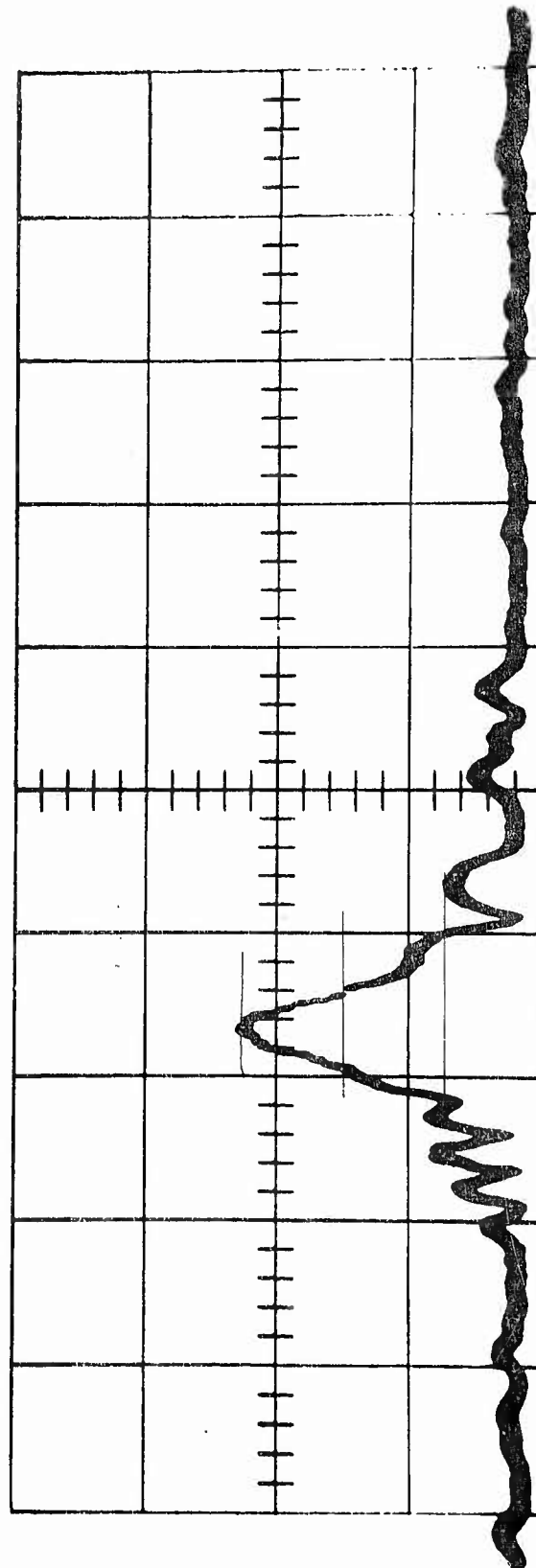
Figure 25. 173 Inch 240 Slot Blade Antenna without Cell Foam

over only one-half of the antenna length. A power distribution measurement was then made at 16.35 KMC and the distribution, while asymmetrical to some degree, did include the whole antenna.

Two other factors which might cause degradation of the azimuth beamwidth were also suspected. The trailing edge wedge is thicker at one end than at the other, and this can cause some phase distortion. A slight curvature in the antenna would produce a similar result.

If only slight defocusing were the reason for the poor beamwidth, then a severely tapered power distribution would restore both good beamwidth and reasonable sidelobes. If phase distortion is too bad, power tapers alone will not help; this was not expected to be the case.

The trailing edge of the blade was removed and the slot lengths were modified to provide a Taylor power distribution for 40 db sidelobes in the presence of the trailing edge. A new test was run yielding 20 db sidelobes and a 0.28 degree beamwidth when measured at a range of 1600 feet. The results are shown in Figure 26.



Scale Factor =  $1.1^{\circ}/\text{CM}$

Figure 26. Azimuth Pattern for 173 Inch 240 Slot Blade Antenna

#### IV. THE BLADE-HUB ASSEMBLY

A UH-1B hub with a radar waveguide installed to transmit energy from the cabin to the blade is shown in Figure 27. The waveguide must be free to accommodate rotational motion, control motion, and stabilizer bar motion. In the UH-1B, control motions consist of  $\pm 12^\circ$  flapping (see-saw motion), 0 to 10 degrees of collective pitch change,  $\pm 25$  degrees of cyclic pitch change. Stabilizer bar motion is very slight.

A fixed standpipe, mounted at the base of the transmission will house the waveguide inside the hollow mast. Rotational motion is taken out at the mast head by a rotating joint. A second rotating joint mounted at  $90^\circ$  to the joint at the masthead, a piece of flexible waveguide, and a rotating joint mounted on the grip permit the flapping motion. Another joint on the grip provides freedom for cyclic pitch change.

All the items used are standard instrumentation and off the shelf radar hardware. The necessary brackets and clamps can be mounted on the hub without any drilling or tapping. The hardware can be either strapped or bonded to the hub.

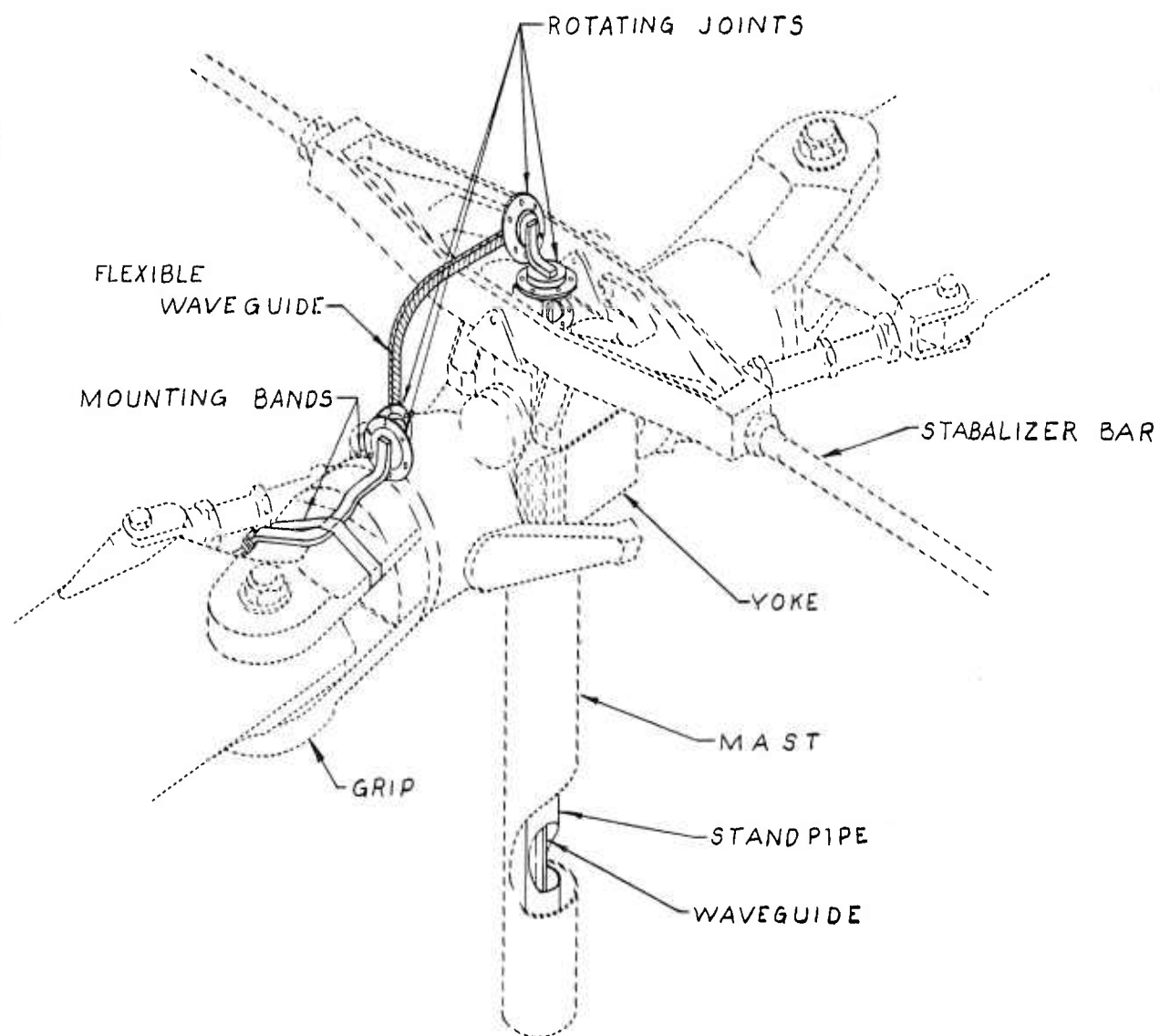


Figure 27. The Blade - Hub Assembly

## V. THE LEADING EDGE BLADE ANTENNA

Placement of the slotted array in the leading edge of the rotor blade was considered under the Company-funded study conducted in early 1963. The idea was rejected at that time because of the erosion that occurs in the leading edge of the blade during rotation. A study of this erosion problem has recently been conducted at Bell with considerable success. Testing is still in progress. Results to date have been:

1. Development of a tape that could be applied to the leading edge which would be good for at least 20 hours.
2. Development of a non-metallic material to replace the stainless steel abrasion strip currently on the leading edge of all UH-1B blades.

As a result, the leading edge antenna configuration now appears practical. Its advantages are:

1. The entire blade length might be used as the antenna.
2. Modification to the blade is almost negligible. The brass nose block would have to be redesigned to accommodate the antenna. The change in the weight and balance of the blade is negligible.
3. Building of flight test blades with the antenna in the leading edge would involve only minor changes in production methods presently employed for the UH-1B blades. Several major changes would be necessary for a trailing edge blade antenna.

A 43-inch blade section has been prepared and the slots are currently being cavitroned (special process using ultrasonic techniques) in the leading edge. This blade will then be tested and the results included as an addendum to this report. Figure 28 shows the leading edge antenna configuration.



## V. THE LEADING EDGE BLADE ANTENNA

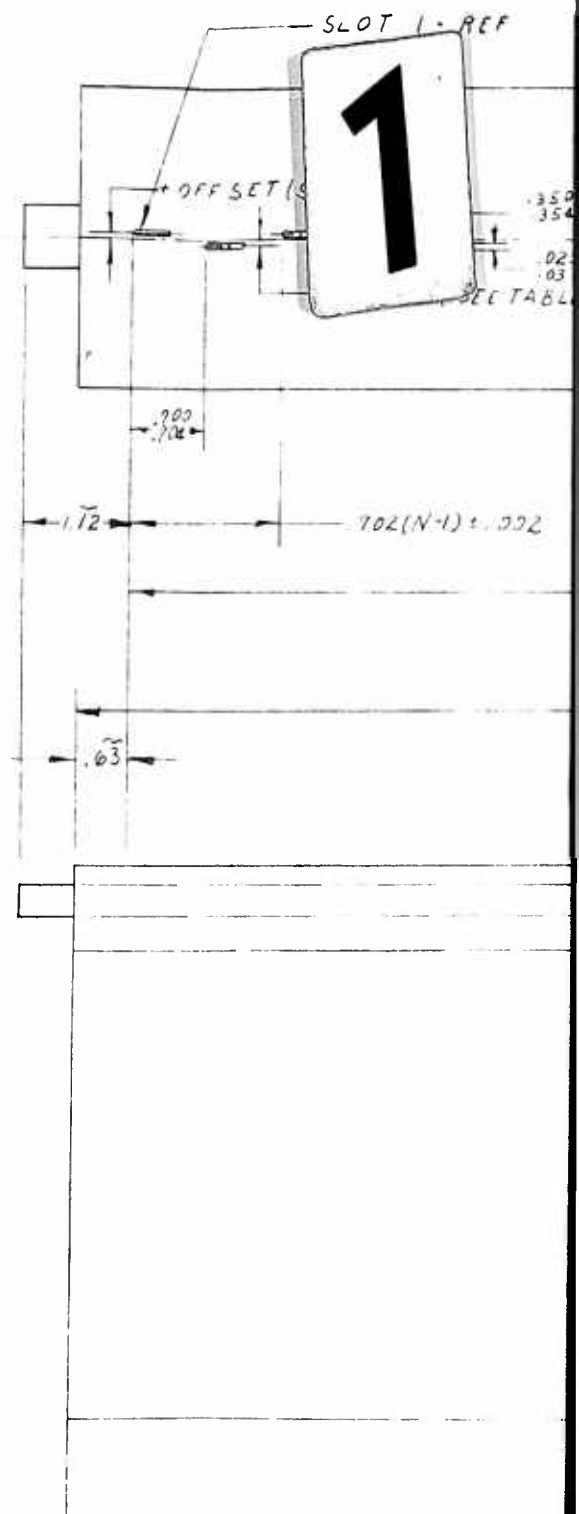
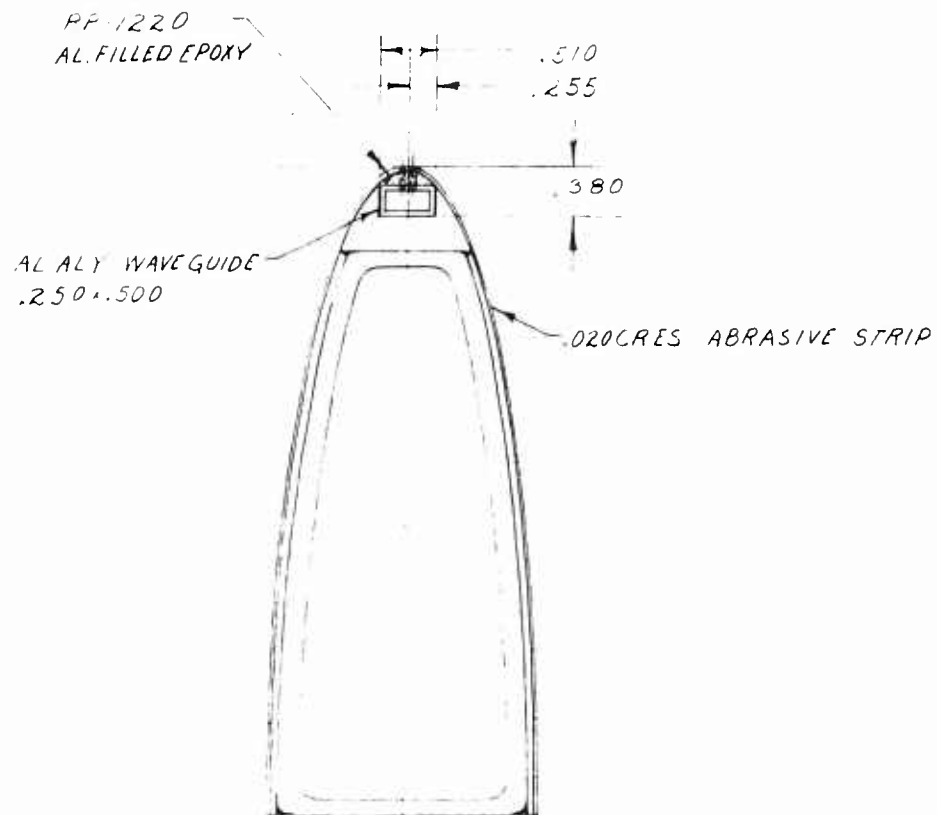
Placement of the slotted array in the leading edge of the rotor blade was considered under the Company-funded study conducted in early 1963. The idea was rejected at that time because of the erosion that occurs in the leading edge of the blade during rotation. A study of this erosion problem has recently been conducted at Bell with considerable success. Testing is still in progress. Results to date have been:

1. Development of a tape that could be applied to the leading edge which would be good for at least 20 hours.
2. Development of a non-metallic material to replace the stainless steel abrasion strip currently on the leading edge of all UH-1B blades.

As a result, the leading edge antenna configuration now appears practical. Its advantages are:

1. The entire blade length might be used as the antenna.
2. Modification to the blade is almost negligible. The brass nose block would have to be redesigned to accommodate the antenna. The change in the weight and balance of the blade is negligible.
3. Building of flight test blades with the antenna in the leading edge would involve only minor changes in production methods presently employed for the UH-1B blades. Several major changes would be necessary for a trailing edge blade antenna.

A 43-inch blade section has been prepared and the slots are currently being cavitroned (special process using ultrasonic techniques) in the leading edge. This blade will then be tested and the results included as an addendum to this report. Figure 28 shows the leading edge antenna configuration.



2

SLOT 1 - REF

OFFSET (SEE TABLE)

.350  
.354 TYP

.020  
.031 TYP

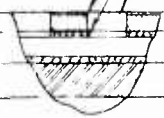
OFFSET (SEE TABLE)

.002  
.002

$10L(N-1) \pm .002$

NO BURRS

TYPICAL SLOT



TOLERANCES

.X = ±.1

.XX = ±.03

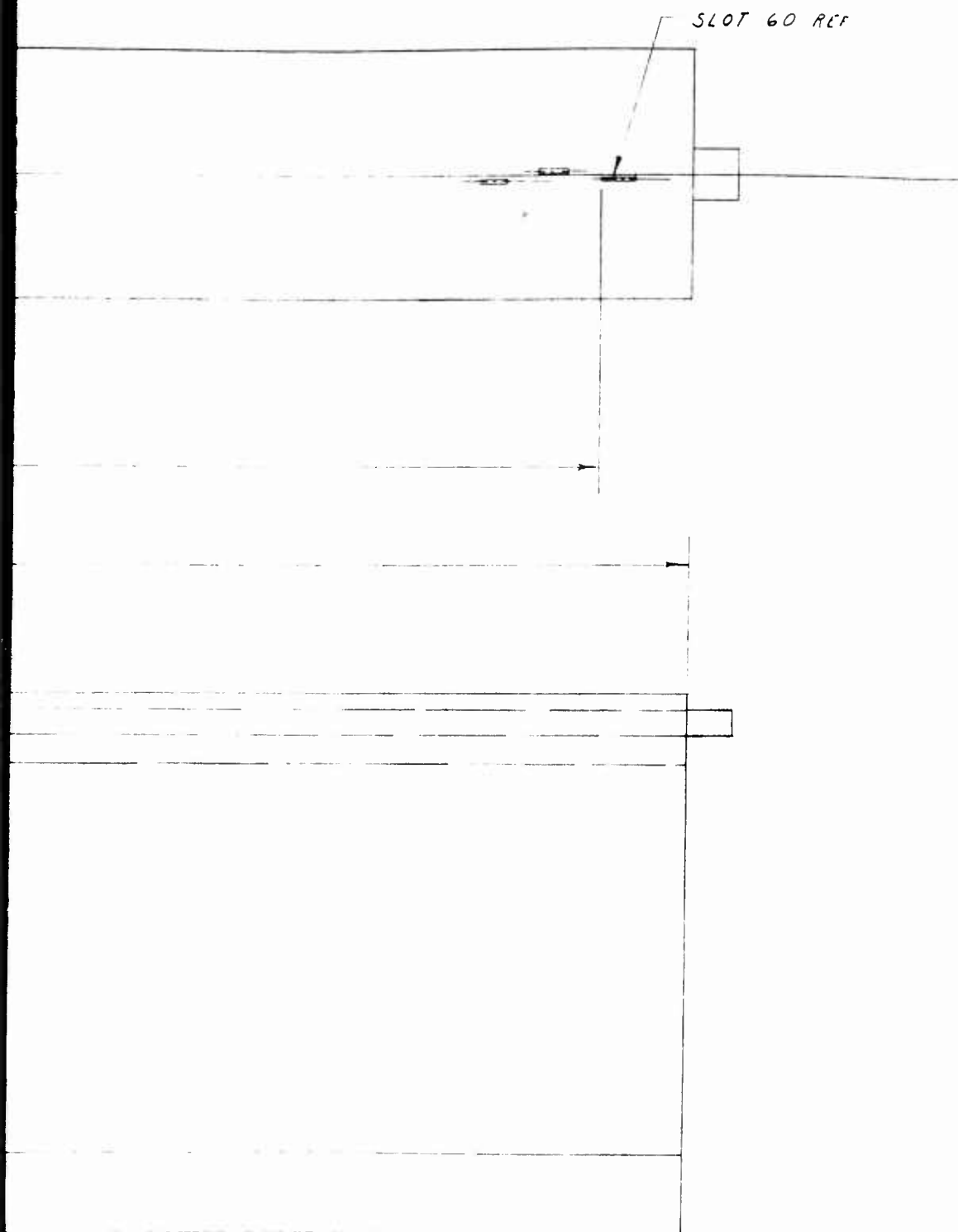
.XXX = ±.010

3

41.416  
41.420

43.0

4



5

TABLE OF OFFSETS $\pm .001$			
SLOT	OFFSET		
1	+ .018	31	+ .115
2	- .019	32	- .120
3	+ .019	33	+ .125
4	- .020	34	- .130
5	+ .021	35	+ .136
6	- .023	36	- .141
7	+ .025	37	+ .147
8	- .027	38	- .152
9	+ .030	39	+ .158
10	- .032	40	- .164
11	+ .035	41	+ .170
12	- .039	42	- .176
13	+ .042	43	+ .181
14	- .045	44	- .184
15	+ .049	45	+ .185
16	- .052	46	- .183
17	+ .056	47	+ .177
18	- .060	48	- .170
19	+ .064	49	+ .161
20	- .068	50	- .152
21	+ .071	51	+ .143
22	- .075	52	- .133
23	+ .079	53	+ .124
24	- .084	54	- .115
25	+ .088	55	+ .107
26	- .092	56	- .101
27	+ .097	57	+ .095
28	- .101	58	- .091
29	+ .106	59	+ .088
30	- .111	60	- .087

Figure 28.  
Drawing of the Leading Edge Blade Antenna

## VI. CONCLUSIONS

It appears as though usable antennas of great length can be located in any one of three locations in the rotor blade. The two most promising locations are the leading and trailing edges of the rotor blade. Only the trailing edge has been given a full scale radiation pattern test with a 15 foot blade section containing a slotted array antenna.

Two kinds of errors must be considered for either the trailing edge or the leading edge blade antenna design. They are phase and power distribution errors. If the density of the material at the aperture of the antenna is modified, the leak rate and thus the amplitude of the distribution will be modified, resulting in poorer sidelobe values and sidelobe asymmetry. If there are changes in path length between the antenna and the trailing edge of the blade, and if this change is not linear from one end of the antenna to the other, radiation pattern distortion results. These factors, along with dimensional control, are the most important parameters which must be considered in the design of a rotor blade antenna.

It was determined early in the program that perpendicular polarization was required for the trailing edge, to minimize aperture blockage caused by the all metal trailing edge. However, in the case of the leading edge and in the case of the trailing edge where no metal is employed, parallel polarization could be used; however, it is difficult to use with a small waveguide such as  $K_q$  (0.5 x 0.25 inch outside dimension). Since the antenna operates in the  $K_u$  band, inclined shunt slots (parallel polarization) would couple little power from the waveguide. There are, of course, other possibilities for generating parallel polarization, but

most of this antenna development has employed longitudinal slots in the broad face of the guide.

Several single slot, two 60-slot and one 240-slot blade antennas have been built. All except the 60-slot leading edge antenna have been tested. Results indicate that a rotor blade antenna of 175 inches in length can be designed with a beamwidth of approximately  $1/4$  degree. Experience indicates that care must be used in both the design and manufacture of the assembly to ensure end quality.



APPENDICES

## ADDENDUM I

### Rotor Blade Deflection (Drag) Tolerances for Microwave Beams

The following table can be compared with deflection curves, (see Figure 29) and a sketch of the actual in-plane blade deflections for usable sectors of scan and antenna lengths, thus determining maximum usable frequency and resolution as a function of sector scan angle. As an example, a  $K_u$  band antenna could effectively use approximately 15 feet of the rotor blade length for a full  $360^\circ$  of scan, or more blade length by limiting the scan angle. The maximum deflection allowed for the radiating part of the antenna is one-fourth of the operating wavelength. In the microwave table below are listed several typical microwave frequency bands and the one-fourth length in inches for each. Again, improvement in resolution (smaller beamwidth) is directly proportional to antenna length.

<u>Frequency Band</u>	<u>Frequency In mc/s</u>	<u>Wavelengths (in inches)</u>	<u>Permissible Deflection (In Inches)</u>
S	3,000	3.94	0.98
X	10,000	1.18	0.30
$K_u$	16,000	0.716	0.18
$K_a$	35,000	0.338	0.084
V	75,000	0.157	0.039

# IN-PLANE BLADE DEFLECTION CURVES AT VARIOUS AZIMUTH POSITIONS

$V_{TRUE} = 126$  KNOTS (STABILIZED LEVEL FLIGHT)

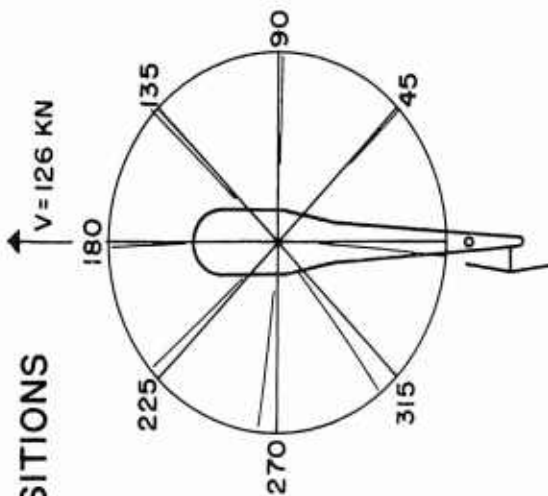
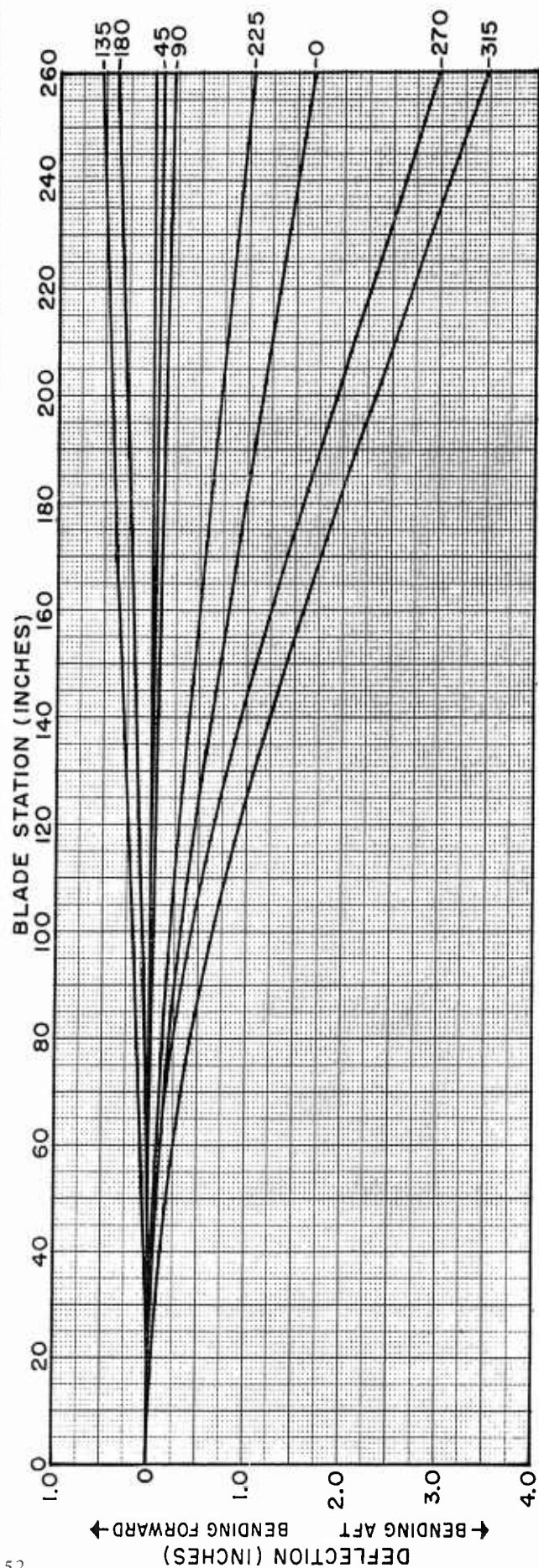


Figure 29.



TOP VIEW OF HELICOPTER  
SHOWING AZIMUTH POSITIONS



## ADDENDUM II

### Range Limit Due to Rotor Speed

With a one-fourth degree beam scanning  $360^\circ$  five times/second, such a beam will move one beamwidth in  $1/7200$  seconds or 139 microseconds, equivalent to a range of about 14 statute miles. One might expect a more difficult condition, but a 5 cycle scan is not a very rapid one. If six beams were used to increase the selector scan rate to 30 frames/second, since there are six individual beams, there is no decrease in the maximum range. The radar signal must get out to the target and back to the antenna before the antenna has moved one beamwidth or the radar will be range limited due to the scanning rate.

At least one pulse must be transmitted per beamwidth during the scan and more are preferred. One pulse per beam at 5 cycles per second would require a PRF of 7,200 pulses/second. 14,000 to 28,000 pulses/second would be more desirable.

### ADDENDUM III

#### Pulse Width Aperture Limiting

A limitation on the maximum length of a usable rotor blade antenna may be pulse width limiting. If a slot array antenna of the rotor blade type is fed from one end, it must be assumed that the pulse width is sufficiently great such that power is still being radiated from the first slot when the last slot begins radiating microwave power. The antenna may be fed from the center, but pulse width antenna aperture limiting must be considered. A conventional pulse width is one-tenth microsecond. Microwaves travel approximately 100 feet in free space during that time period. Shorter pulses are even more desirable from the standpoint of range resolution. A 0.1 microsecond pulse provides a 50 foot range resolution. Microwaves travel slower in a waveguide than in free space, depending on the waveguide material and dimension. A 0.020 microsecond pulse could not be used with an end-fed slot array which is 44 feet long. However, long rotor blade antennas can be used effectively with good range resolution.

#### ADDENDUM IV

##### The Rayleigh Range and Beamwidth

The significance of the Rayleigh Range is that the often referred far field beamwidth may not be a satisfactory description of the antenna resolution, when beam measurements are to be made within the Rayleigh Range. However, the antenna can be focused. Normally, antennas are focused at infinity or beyond the Rayleigh Range, but with an antenna as large as the example, it may well be an advantage to focus the antenna inside the Rayleigh Range.

Side-looking radars with long antennas (a 15 foot length is typical) using conventional signal processing (simply photographing one line or one beam at a time) are not usually concerned with targets so very close. Close targets are of concern when using a helicopter. Since the side-looking radar does not scan, if the antenna were focused, it could only provide one spot of the terrain or one line at a time. If the rotor blade antenna were focused with the antenna scanning, not only a spot could be recorded, but a line  $360^\circ$  about the helicopter. However, the focusing is not as abrupt as suspected (a scale drawing should be used). How sharp a focus can be achieved? The beam may be focused (much like a flashlight and lens) to a spot one foot wide at a range of 229 feet. This would be a remarkable resolution, capable of resolving two men, each standing one foot from the other.

Other special techniques may be used to ensure the best performance from the antenna system and computer tests have been conducted at Bell Helicopter Company facility to carefully analyze the antenna field strengths in the near field zone, in the zone of the Rayleigh Range.

Some possibilities of investigation are parallel beams (using the co-incidence as the resultant beam), and multiple beams, some focused at infinity and others focused close to the helicopter. A special application of digital computers for calculating Rayleigh Range field strengths for slot array antennas (the rotor blade antenna) is shown in this report (Addendum V). This method of calculation is expected to be useful in the development of the rotor blade antenna, particularly in the Rayleigh Range region.

## ADDENDUM V

### Computer Programs

Several computer programs were written to examine various aspects of the blade antenna design. The antenna phase pattern and bandwidth were examined for various values of the Rayleigh Range and for three values of slot number. A program was also written using equations reported by Andre Dion (see references). This program computes slot offset, slot conductance, and the amplitude distribution for three different values of frequency.

RADAR 1 - This program computes the antenna phase pattern and bandwidth for the cases  $N = 5$ ,  $50$ , and  $368$  where  $N$  = number of aperture wavelengths. Phase pattern and bandwidth are computed for seven values of distance where the distance is some scale factor times the Rayleigh Range. These values are:

$$R(1) = 4 \times R1$$

$$R(2) = 2 \times R1$$

$$R(3) = R1$$

$$R(4) = 0.5 \times R1$$

$$R(5) = 0.25 \times R1$$

$$R(6) = 0.125 \times R1$$

$$R(7) = 0.0625 \times R1$$

where  $R1$  = Rayleigh Range.

The power radiating from each slot was normalized ( $P1 = 1.0$ ). As a result, the computed pattern is really a phase pattern only. Any amplitude pattern could be superimposed on it without destroying the results. The important parameters in setting up these calculations are shown in Figure 30.



# LAYOUT DRAWING FOR COMPUTER PROGRAMS RADAR 1 AND RADAR 2

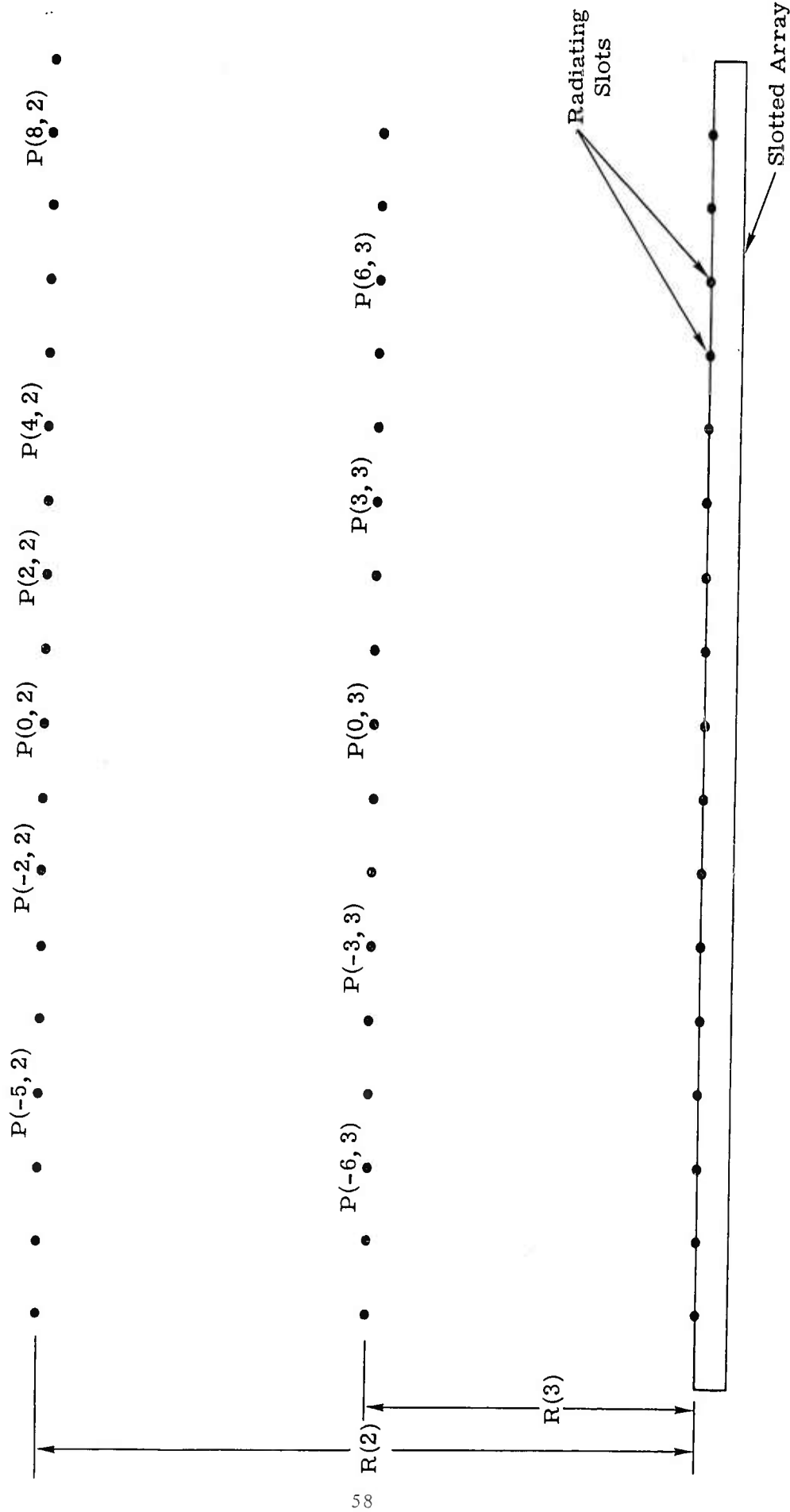


Figure 30 Sketch Showing Variables and Layout for Computer Programs Radar 1 and Radar 2

K = Point at which power measured

J = Particular value of the Rayleigh Range  
(example J = 3; R(J) = R1)

P(K,J) = Power at J<sup>th</sup> value of the Rayleigh  
Range and at K<sup>th</sup> value along the  
antenna

S = Total number of slots for the antenna  
where S = 2N + 1

The bandwidth is measured by ALPHA ( $\alpha$ ). The value of real interest is that value of K for which  $\alpha = 3\text{DB}$ . This corresponds to the half power point.

Values for GAMMA ( $\gamma$ ) and DELTA ( $\delta$ ) were also obtained from this program. Closer examination of these data revealed that no new information was gained by knowing their values.

Although RADAR 1 was set up for the cases N = 5, 50, 368, only the N = 5, and 50 cases were run. The reason for not running the 368 case was computer time required. RADAR 1 was then modified to get results on the N = 368 case in a reasonable time. It became RADAR 2.

RADAR 2 - This program considered only the N = 368 case. Every fourth value of P(K,J) was computed and only the odd values of J were used. Thus, we obtain information for:

$$R(1) = 4 \times R1$$

$$R(3) = R1$$

$$R(5) = 0.25 \times R1$$

$$R(7) = 0.0625 \times R1$$

The P(K,J) values computed are P(0,J); P(4,J), P(8,J).....P(368,J).

For both RADAR 1 and RADAR 2, only one-half the pattern was actually computed. Because of symmetry the pattern for negative values of K is exactly like that for positive K values.

Basic equations and terms for RADAR 1 and RADAR 2:

N = Number of aperture wavelengths

S = Number of slots =  $2N + 1$

$\cos \delta_n$  = Phase front

$\lambda$  = LAMBDA = 0.717 inches corresponding to

f = FREQUENCY = 16.50 KMC

$\Delta_n = A \frac{1 - \cos \theta_n}{\cos \theta_n}$  for  $n = 1, 2, 3, \dots, N$

THETA =  $\theta_n = \tan^{-1} \frac{n}{R}$  where  $R = R(J)$  and  $n = 1, 2, 3, \dots, N$

$A = \frac{R}{\lambda} (360^\circ)$

$D = N\lambda$

$R_1 = \text{Rayleigh Range} = D^2/2\lambda$

RADAR 3 - This program computes slot offset, slot conductance, and the amplitude distribution for three values of frequency.

FREQ (1) = 16.15 KMC	$\lambda_{FS} (1) = .7313''$	$\lambda_g (1) = 1.4924''$
FREQ (2) = 16.25 KMC	$\lambda_{FS} (2) = .7269''$	$\lambda_g (2) = 1.4552''$
FREQ (3) = 16.50 KMC	$\lambda_{FS} (3) = .7158''$	$\lambda_g (3) = 1.3738''$

where

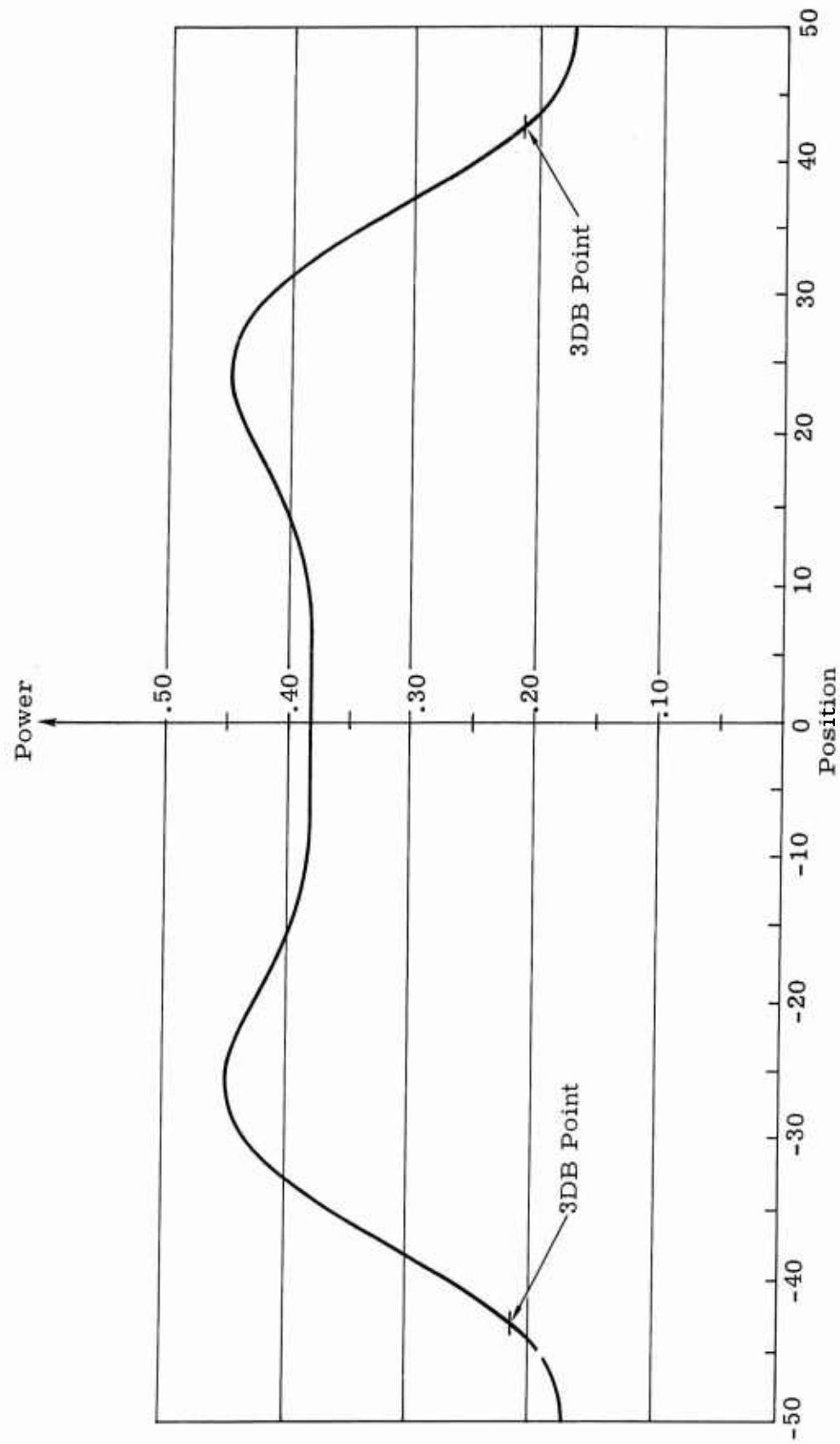


Figure 31. Antenna Phase Distribution at 4 Times the Rayleigh Range for  $N = 50$

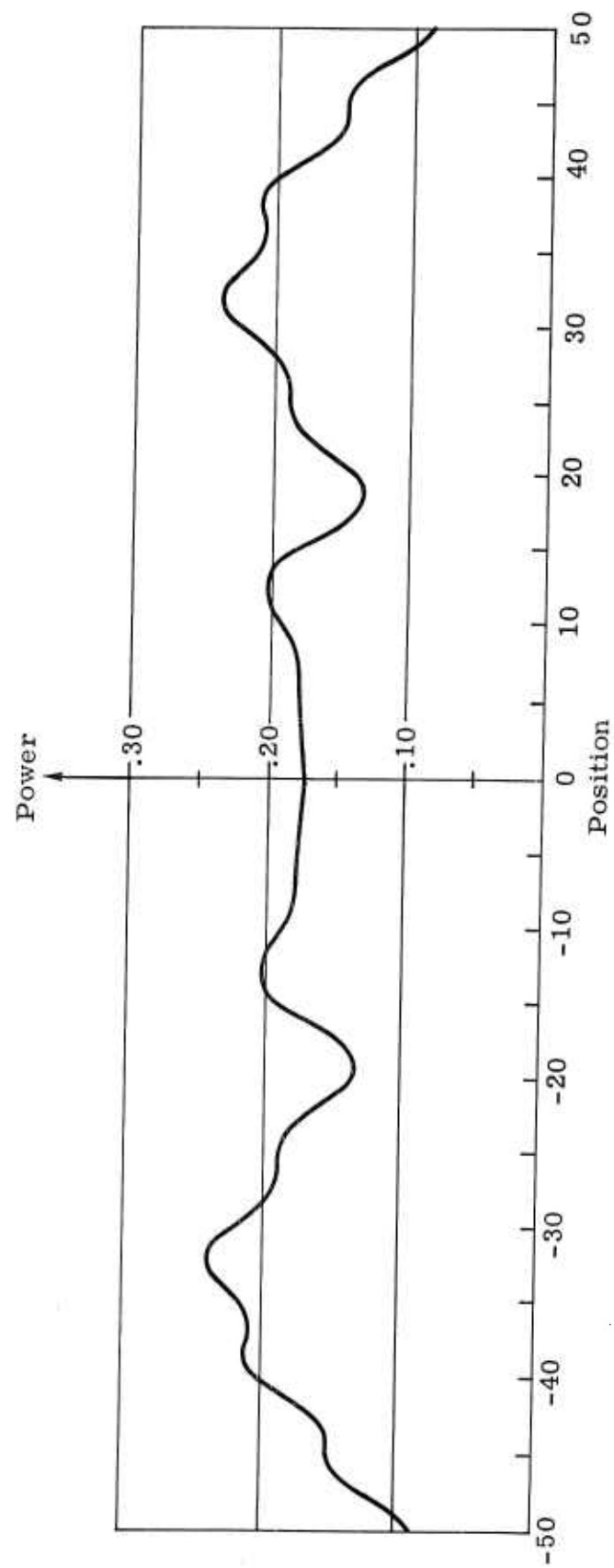


Figure 32. Antenna Phase Distribution at the Rayleigh Range for  $N = 50$

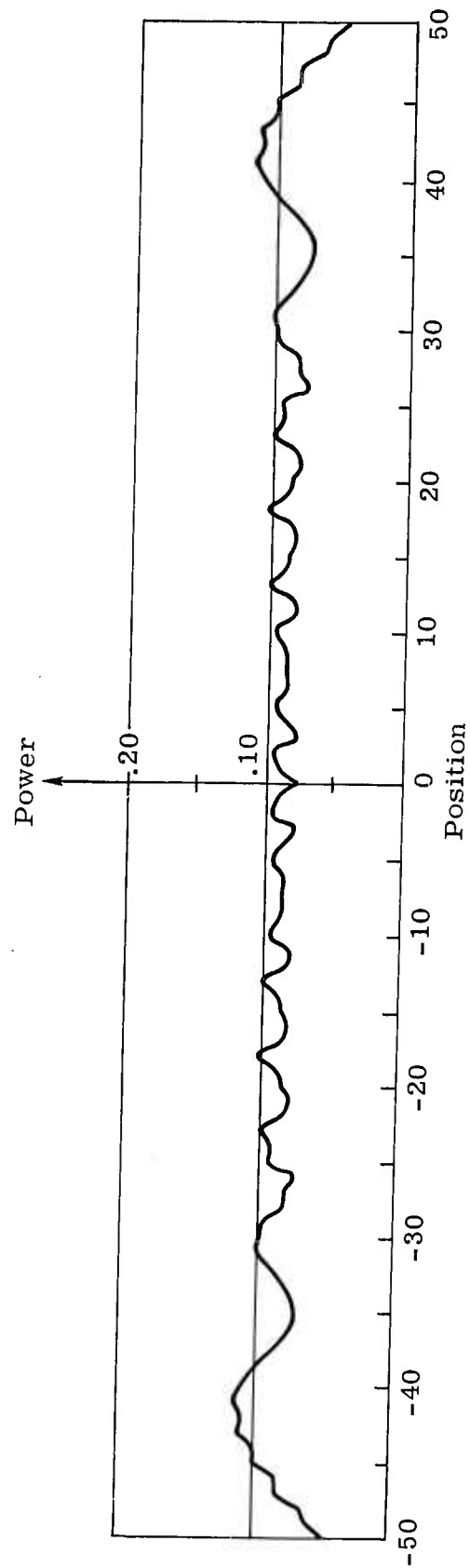


Figure 33. Antenna Phase Distribution at  $1/4$  of the Rayleigh Range for  $N = 50$

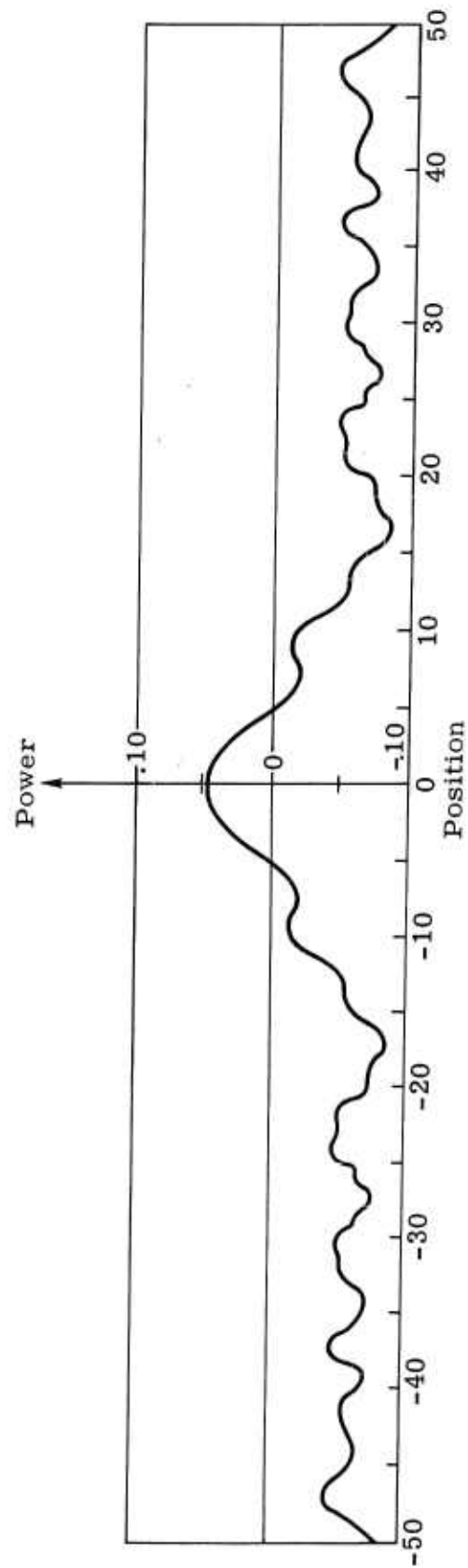


Figure 34. Antenna Phase Distribution at  $1/16$  of the Rayleigh Range for  $N = 50$

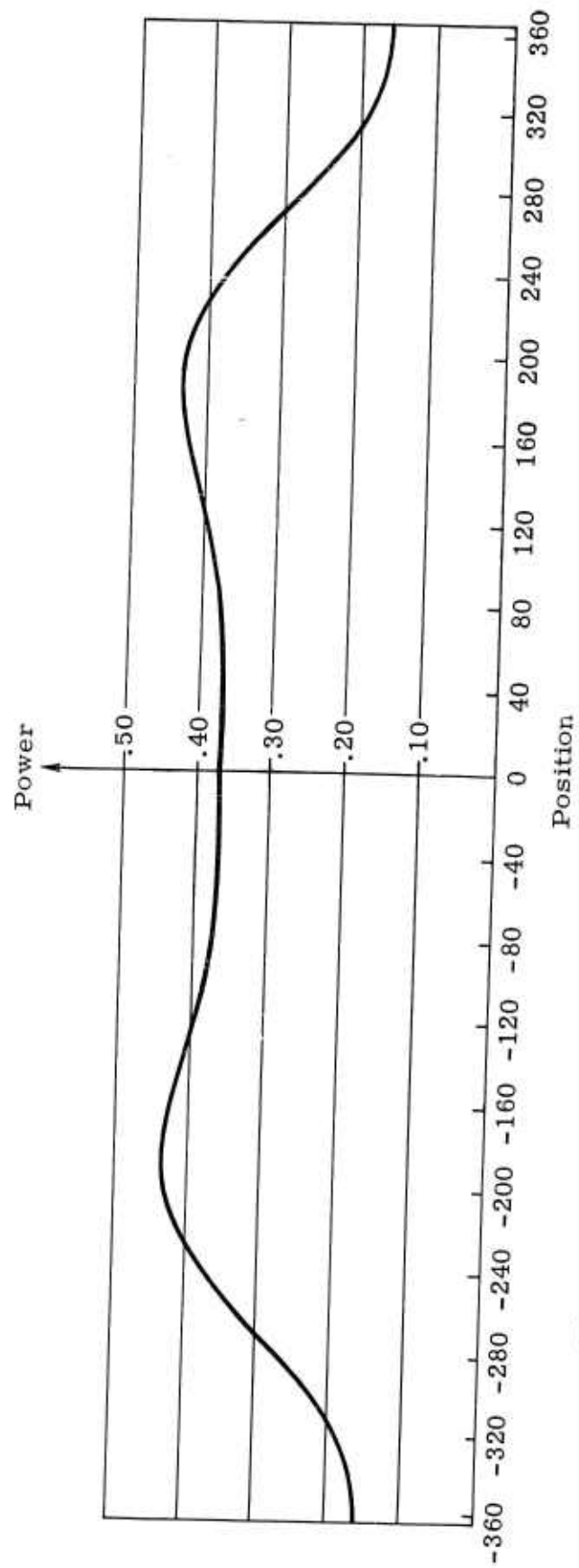


Figure 35. Antenna Phase Distribution at 4 times the Rayleigh Range for  $N = 368$



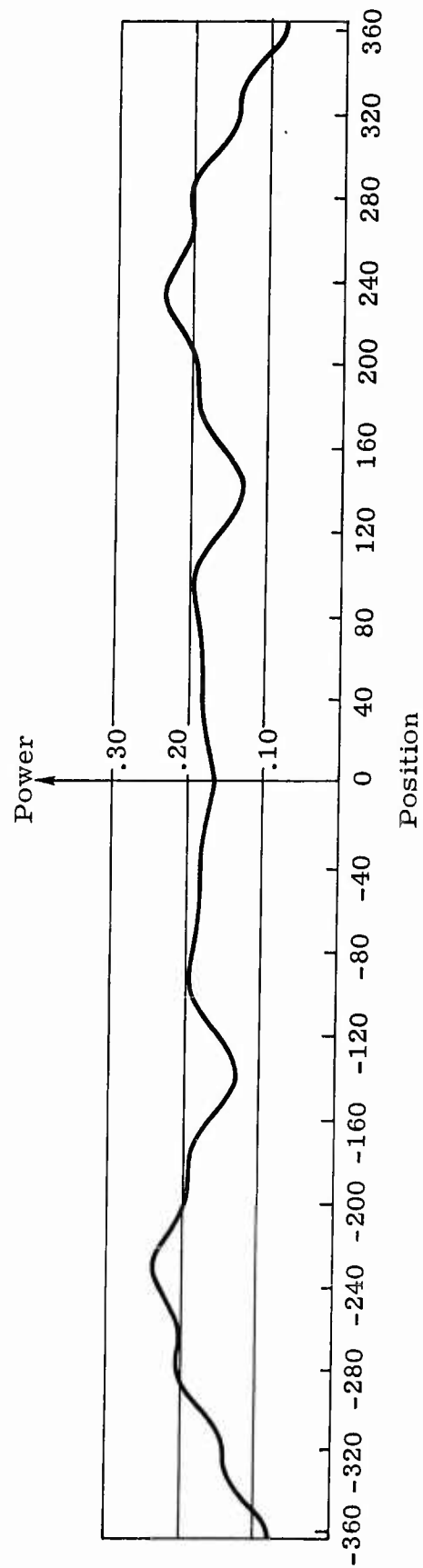


Figure 36. Antenna Phase Distribution at the Rayleigh Range for  $N = 368$ .

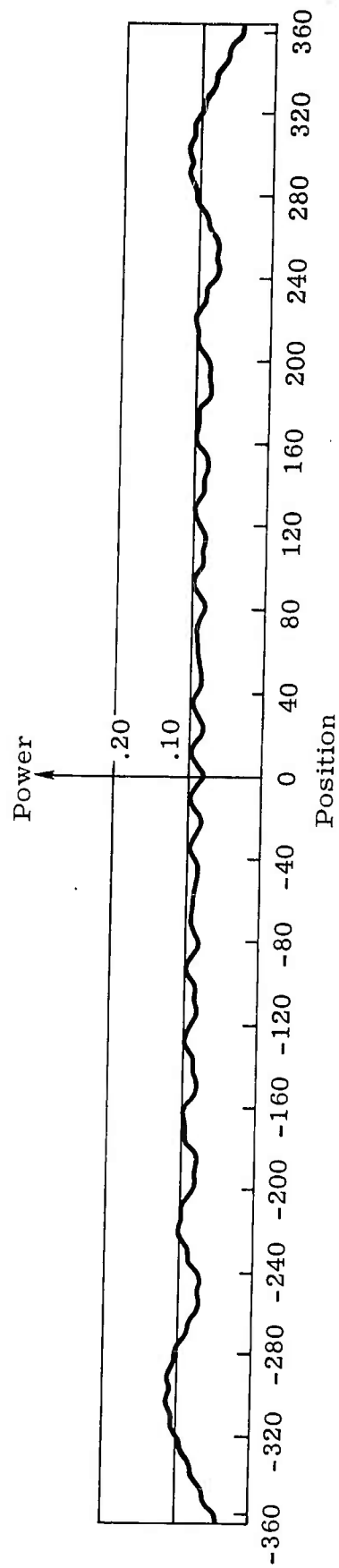


Figure 37. Antenna Phase Distribution at  $1/4$  of the Rayleigh Range for  $N = 368$

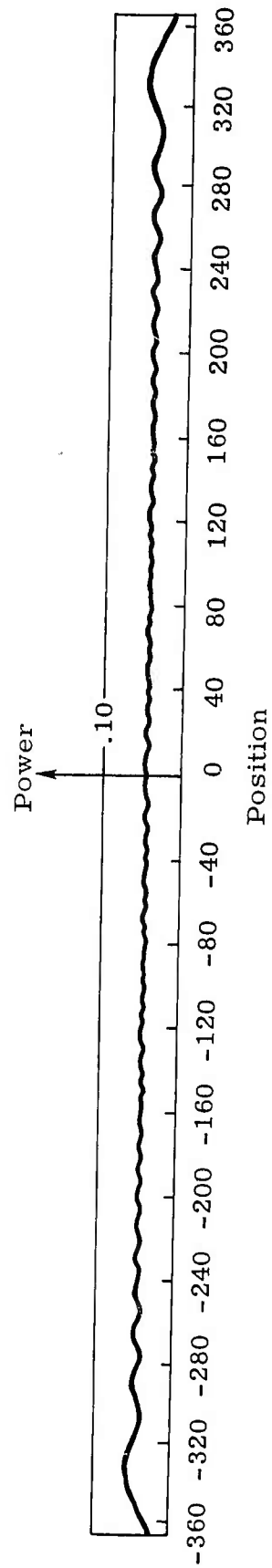


Figure 38. Antenna Phase Distribution at 1/16 of the Rayleigh Range for N = 368

$\lambda_{FS}$  = LAMBDA (FREE SPACE) = free space wavelength in inches

$\lambda_g$  = LAMBDA (WAVEGUIDE) = waveguide wavelength in inches

$F(P)$  = Amplitude at  $P^{th}$  value along antenna

$LG(P)$  = Normalized slot conductance per unit length of antenna  
times one-half of the antenna length.

$Y(P)$  = Offset of slot from centerline of antenna.

Antenna length =  $2L$

This program was run for a 21-slot antenna to check the results reported by Andre Dion (see references). Knowing that Dion's results for the 21-slot case are correct, information for the 240-slot antenna can be extracted from his reported curves. After checking the value of conductance, the slot offset was computed using Stevenson's formula with an amplitude pattern for 30 db sidelobes and 5 per cent power to the load.

Phase pattern plots for various values of the Rayleigh Range are shown in Figures 31 through 38. Plots are given for both the  $N = 50$  and  $N = 368$  cases. A close correspondence between the  $N = 50$  and  $N = 368$  cases can be noted at the Rayleigh Range or greater. This distance would correspond to the far field region of the antenna.

At one-fourth of the Rayleigh Range the phase patterns for  $N = 50$  and  $N = 368$  are similar, but the  $N = 368$  array produces a smoother pattern. Power levels are the same. At one-sixteenth of the Rayleigh Range the  $N = 50$  phase pattern has started to fall off on either side of the symmetry axis; however, for the  $N = 368$  array a very smooth distribution results.

Figures 39 and 40 show plots done for the Dion program. In Figure 39

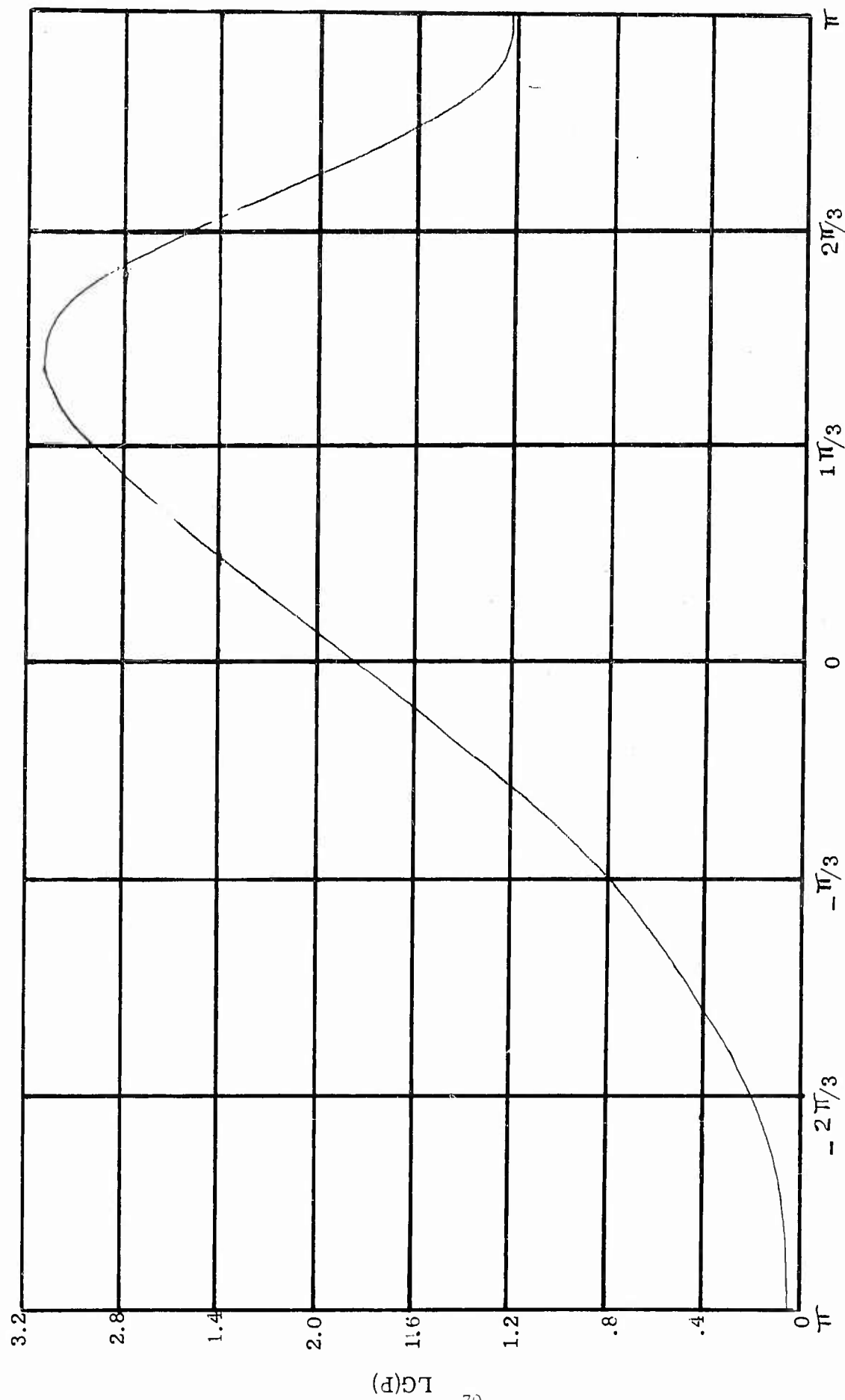


Figure 39. Plot of Normalized Slot Conductance for a 241 Slot Array having 30 db Sidelobes and 5% Power to the Load

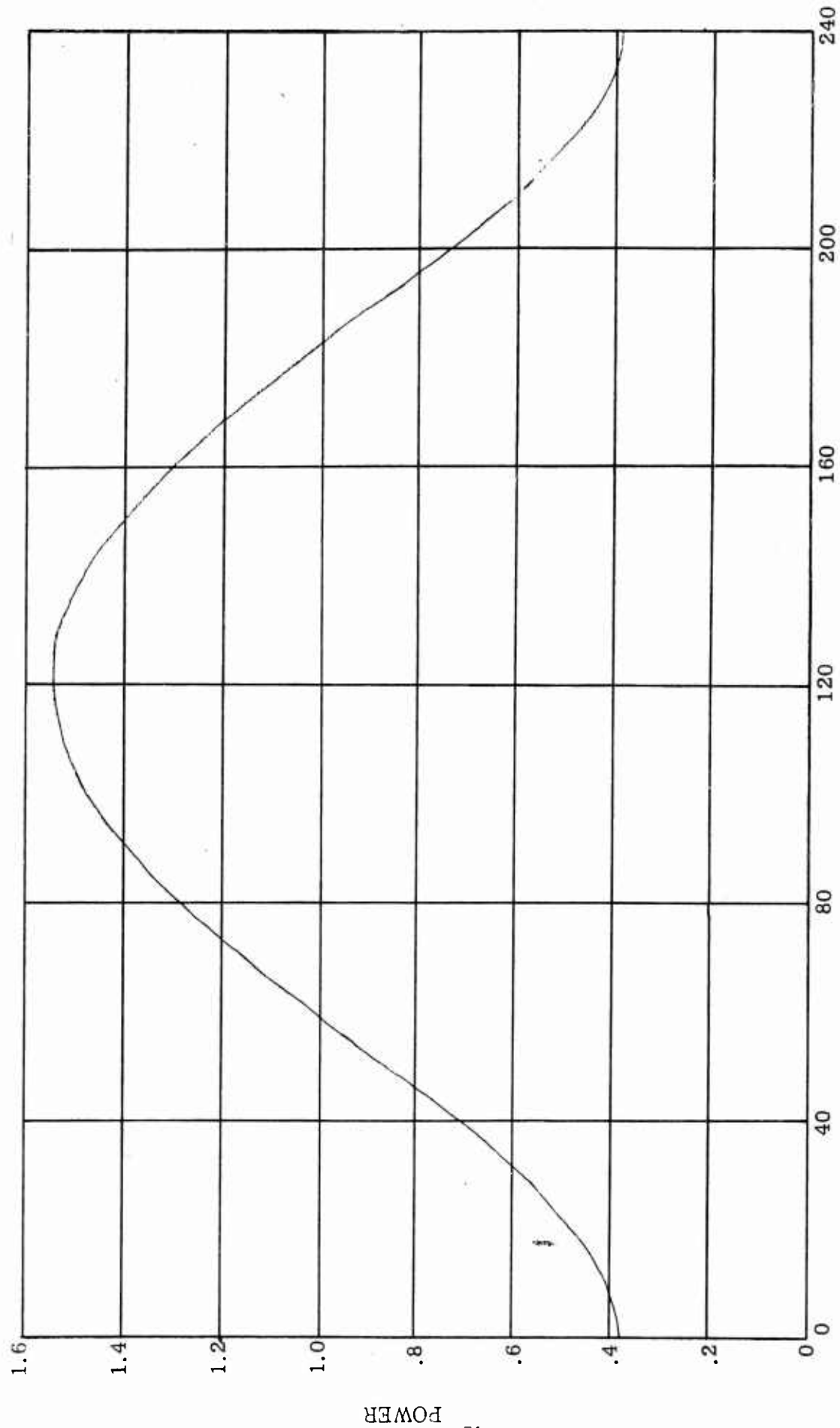


Figure 40. Plot of Amplitude Distribution of a 240 Slot Array Range for  $N = 368$

normalized slot conductance for a 241-slot array having 30 db sidelobes and 5 per cent power to the load is plotted. The conductance of any slot may be found by dividing the abscissa between  $-\pi$  and  $+\pi$  into a number of spacings equal to the total number of slots minus one. Then read the corresponding ordinate and divide by one-half the total number of slots.

The amplitude distribution for a 241-slot array having 30 db sidelobes is shown in Figure 40. This is a distribution computed using results reported by T. T. Taylor (see references).

#### VIII. REFERENCES

1. Barlin, L. L., Pattern Build-Up as a Function of Time in 10 Element Arrays, Microwave Engineers Handbook and PGAP, 1963.
2. Blankenship, B. L. and Harvey, K. W., A Digital Analysis for Helicopter Performance and Rotor Blade Bending Moments, Journal of the American Helicopter Society, Vol. 7, No. 4, October, 1962.
3. Dion, Andre, Nonresonant Slotted Arrays, IRE Transactions on Antennas and Propagation, Vol. AP-6, October 1958, pp 360-9.
4. Jasek, H., Antenna Engineering Handbook, McGraw Hill Book Company, 1961
5. Ramsay, J. F., Parallel Beam Antennas, Space Aeronautics R & D Handbook, 1960-61.
6. Sherman, John W., Properties of Focused Apertures in the Fresnel Region, IRE Transactions on Antennas and Propagation, July 1962.
7. Sherman, John W., Some Comments on the Transmission of Power by the Use of Microwave Beams, IRE Transactions on Antennas and Propagation, November 1961, p 580.
8. Silver, S. (ed), Microwave Antennas Theory and Design, MIT Radiation Laboratory Series, Vol. 12, McGraw Hill, New York, 1949.
9. Slater, J. C. and Frank, N. H., Introduction to Theoretical Physics, McGraw Hill, New York
10. Taylor, T. T., Design of Line Source Antennas for Narrow Beamwidth and Low Sidelobes, IRE Transactions on Antennas and Propagation, AP-3, January 1955, pp 16-23.



# IX. DISTRIBUTION LIST

Capt. J. E. Perry (RAAV-9)  
Chief, Bureau of Naval Weapons  
Room 1W98, W Building  
Washington 25, D.C. (3)

Lcdr. J. Charles  
Life Sciences Department  
Point Mugu, California

Commanding Officer  
USAE LRDA  
Attn: SELRA/SRI (Mr. R. R. Hefter)  
Fort Monmouth, New Jersey

ODDR&E Office of Electronics  
Attn: Cdr. W. W. Vallandingham, USN  
Pentagon (Room 3D1037)  
Washington 25, D.C.

Mr. H. Birmingham  
U. S. Naval Research Laboratory  
Washington 25, D.C.

Commanding Officer  
Office of Naval Research Branch Office  
Box 39, Navy #100, Fleet Post Office  
New York, New York

Commanding Officer  
USAE LRDA  
Attn: SELRA/SRI (Mr. S. J. Zywtow)  
Fort Monmouth, New Jersey

Commanding Officer  
Office of Naval Research Branch Office  
207 West 24th Street  
New York 11, New York

Mr. L. S. Guarino  
Airborne Instrument Laboratory  
Commanding Officer  
U. S. Naval Air Development Center  
Johnsville, Pennsylvania

Commanding Officer  
Office of Naval Research Branch Office  
1000 Geary Street  
San Francisco 9, California

Lcdr. D. E. Rosenquist, USN, Code 461  
Chief of Naval Research  
Room 2609, T-3 Building  
Washington 25, D.C. (10)

Federal Aviation Agency  
Information Retrieval (MS-112)  
Washington 25, D.C.

Commanding Officer  
Office of Naval Research Branch Office  
495 Summer Street  
Boston 10, Massachusetts

Chief of Research & Development  
Department of the Army (CSRD/D)  
Washington 25, D. C.

Commanding Officer  
Office of Naval Research Branch Office  
86 East Randolph Street  
Chicago 1, Illinois

Commanding Officer  
Transportation Res. & Engr. Command  
Attn: Aviation Divisions  
Ft. Eustis, Virginia

Commanding Officer  
Office of Naval Research Branch Office  
1030 East Green St.  
Pasadena 1, California

Commander  
Hq. Air Force Systems Command  
Andrews AFB, Maryland

Mr. W. C. Robinson  
AMCRD/DE-E  
Electronics Division  
R&D Directorate  
Army Materiel Headquarters  
Washington 25, D.C.

Commandant  
School of Aviation Medicine, USAF  
Randolph AFB, Texas  
Attn: Research Secretariat

Chief, Engr. Electronics Section  
National Bureau of Standards  
Washington 25, D.C.

DISTRIBUTION LIST (CONT'D)

U. S. Naval Training Devices Center Pt. Washington, L.I., N.Y. Attn: Joe N. Pecoraro Head, Equip. Res. Div.	Commanding Officer AMSEL-AV Ft. Monmouth, New Jersey
Hq. Quartermaster Res & Engr. Command Quartermaster Res. & Engr. Center Natick, Massachusetts	Commanding Officer SELHU USA Res. & Dev. Activity Fort Hauchaca, Arizona
Defense Documentation Center Cameron Station Alexandria, Virginia (10)	AMSMD-R Headquarters, Mobility Command Center Line Michigan
British Defense Research P. O. Box 680 Benjamin Franklin Station Washington, D.C. (3)	National Aeronautics & Space Admin. 1520 H Street Code RBB Washington 25, D.C. Attn: Mr. Lowell Anderson Division of Research
Defense Research Member Canadian Joint Staff 2450 Massachusetts Ave., N.W. Washington 8, D.C. (3)	Director Naval Research Laboratory Washington 25, D.C. Attn: Tech. Info. Office
Commanding Officer SELRA/SS Fort Monmouth, New Jersey	AMCRD-DE-MO Headquarters, USA Material Command Washington 25, D.C.
Commanding Officer USAE LRDA Fort Monmouth, New Jersey Attn: SERRA/SRI (Mr. T. E. Maloney)	Commanding Officer U.S. Army Transportation Research Command Attn: Human Factors & Survivability Group
Mr. John Grey Aviation Board Fort Rucker, Alabama	Ft. Eustis, Virginia 23604